

UK UNLIMITED

ATOMIC WEAPONS ESTABLISHMENT

AWE Report No. O 1/97

The Novaya Zemlya Seismic Disturbance  
of 16 August 1997

D Bowers  
Mrs H Trodd  
A Douglas

Recommended for issue by:

A Douglas, Head, Division of Forensic Seismology

Approved for issue by:

DKK Landeg, Project Contract Manager

UK UNLIMITED

## SUMMARY

A small seismic disturbance on 16 August 1997 was located by the Prototype International Data Centre (PIDC) in the vicinity of Novaya Zemlya, the region of a known Russian nuclear test site. Reports in the press suggest that the disturbance may be a low-yield Russian nuclear test, apparently based on observed seismograms that show characteristics typical of underground explosions. Measurements of  $P$  arrival times at 8 stations are consistent with the reported PIDC location in the Kara Sea, about 115 km to the south-east of the test site. The azimuthal distribution of stations suggests that the location of the 16 August disturbance is unlikely to be at the test site. Three-component high frequency  $S/P$  ratios at Kevo, Finland, from the 16 August disturbance, differ from those observed at the same station from four explosions at the test site. Further, the  $S/P$  ratios, and the comparatively impulsive  $S$  onset on the tangential component, from the 16 August disturbance are similar to those predicted from waveform modelling using an earthquake source. Also,  $P$  at NORSAR, Norway, from the 16 August disturbance is remarkably similar to that from the 1 August 1986 Kara Sea earthquake, while being different from  $P$  from a presumed explosion at the test site on 26 August 1984. The remarkable similarity of  $P$  at NORSAR from the 1986 earthquake and the 16 August disturbance, suggests that the two disturbances have a similar location and mechanism. Estimates of the body wave magnitude,  $m_b$ , based on the relative amplitudes of  $P$  observed at NORSAR suggest a maximum likelihood  $m_b$  of about 3.3.

## 1. INTRODUCTION

At around 02:11 UTC on the 16 August 1997 there was a seismic disturbance in the vicinity of the northernmost of the two test sites at Novaya Zemlya (NNZ) (Figure 1a).  $P$  signals from the disturbance were detected by five of the stations that report to the Prototype International Data Centre (PIDC). The epicentre published by the PIDC in the Reviewed Event Bulletin (REB, Table 1 and Figure 1a) is in the Kara Sea about 115 km south-east of NNZ.  $P$  arrival times from three other stations were subsequently obtained. The epicentre estimated from all 8 stations (the position of the stations is shown in Figure 1b) differs little from that published in the REB. As the uncertainties in the epicentre estimates are about 10 km there seems to be little doubt that the disturbance was not at or near NNZ, but out to sea and thus is likely to be an earthquake. The location of the 16 August disturbance reported by the Preliminary Determination of Epicentres (PDE), and from a Joint Epicentre Determination (JED) using regional  $P$  from five NNZ explosions are also given in Table 1. All three estimates of the 16 August epicentre are in the Kara Sea.

However, there have been reports in the press (e.g., Washington Times, 28 August 1997; Guardian, 29 August 1997; International Herald Tribune, 29 August 1997) suggesting that the seismic disturbance of 16 August 1997 was a Russian low-yield nuclear test. Suspicions were raised by the apparent explosion-like characteristics of the observed seismic waveforms. It seems that such press reports of possible low-yield tests are not uncommon (e.g., van der Vink and Wallace, 1996; Ryall et al., 1996). Thus, because the source is in the region of a known test site and the seismic signals are reported as being explosion-like, it was decided to carry out a detailed study of the seismograms to try and identify the source.

## CONTENTS

### SUMMARY

1. INTRODUCTION
2. SOURCE IDENTIFICATION
  - 2.1 Methods of Analysis
  - 2.2 Available Waveform Data
  - 2.3 Discrimination Using Regional Distance Seismograms
  - 2.4 Applying  $S/P$  Ratios as a Discriminant
  - 2.5 Discrimination Using  $P$  Seismograms at NORSAR
  - 2.6 Estimates of the Body Wave Magnitude
3. DISCUSSION
4. CONCLUSIONS
5. ACKNOWLEDGMENTS

### REFERENCES

### NOTE ADDED IN PROOF

APPENDIX A	NORSAR Subarray Beams
A1	16 August 1997 Disturbance
A2	1 August 1986 Kara Sea earthquake
A3	26 August 1984 Presumed Underground Explosion at the North Novaya Zemlya Test Site.

times appear reasonable, except at ARU where no signal is apparent at the expected time. Figure 5 shows vertical-component  $P$  waves from 8 stations recording the 16 August 1997 disturbance, along with the  $P$  arrival time predicted using the REB epicentre and IASPEI 91 tables. Figure 5 also shows the  $P$  onset predicted, using the IASPEI 91 tables, for a hypothetical disturbance located at NNZ (73.33°N, 54.74°E) with origin time 02:11:05.0 UTC (this origin time assumes that the REB onset time at HFS is without error). The predicted  $P$  onset times from the hypothetical NNZ disturbance differ only by a few seconds from those observed at stations in Fennoscandia; however, at NRI and SPITS the predicted  $P$  onset times differ from those reported in the REB by +16.7 and -8.6 seconds respectively. Thus, it is difficult to see how the epicentre of the 16 August disturbance can be at NNZ given the large travel time residuals and azimuthal coverage of the three closest stations KEV, NRI and SPITS (Figure 1b). We suspect that the 'simple' form of the  $P$  waveforms observed at HFS and NORES are those with the explosion-like characteristics reported in the press.

Figures 6a-d present data from stations recording three-component waveforms. The data have been rotated to the usual ray-coordinate system of vertical (Z), radial (R) and tangential (T) directions assuming propagation along the great-circle path from the REB epicentre to the recording station. The data have been filtered using a passband that roughly maximises the signal-to-noise ratio. The  $P$  and  $S$  arrival times predicted from the IASPEI 91 tables are also shown. At FIA0 (the centre element of the FINES array) the  $S/P$  ratio (estimated from the time-domain amplitudes) is less than unity on the Z and R components, but greater than unity on the T-component. The three-components from KAF and KEV are similar, with  $S/P$  ratios significantly greater than unity on the T-component. The Z-component at SPB4 (SPITS) has an  $S/P$  of less than unity, but has  $S/P$  ratios significantly greater than unity on both the R and T components (Figure 6d).

Recordings of  $P$  were also obtained from NORSAR the large aperture array in southern Norway. These are presented in Appendix A, and discussed in a later section of this report.

### 2.3 Discrimination Using Regional Distance Seismograms

Seismograms recorded at regional distances contain many different phases of  $P$  and  $S$  that have been distorted, scattered, and attenuated by the heterogeneous crust, lithosphere and upper mantle. For over 20 years there has been a considerable research effort, especially by US seismologists, directed at understanding the generation and propagation of regional phases. Reviews published in the early 1980's suggest that the  $S/P$  amplitude ratio at 1 Hz is a potentially powerful discriminant between earthquakes and underground explosions. Here  $S$  is taken as the group of phases arriving at, and after, the  $S_n$  phase (a group of phases often referred to as  $L_g$ ). Recently workers have shown that there is a significant improvement in discrimination using  $S/P$  ratios at higher frequencies.

There is a considerable literature on the subject of discrimination using regional phases, but here we refer mainly to a recent review by Blandford (1996). It seems that in general regional seismograms from crustal-depth earthquakes (> 10 km) and deep explosions tend to contain more  $S$  energy at higher frequencies than shallow explosions.

There have been failures of the high frequency  $S/P$  discriminant. Thus, Walter, Mayeda and Patton (1995) show that NTS explosions in high gas porosity materials are indistinguishable from shallow (< 10 km) earthquakes. Blandford (1996) cites recent work that demonstrates that for

## 2. SOURCE IDENTIFICATION

### 2.1 Methods of Analysis

To apply the most reliable identification criteria is difficult. The REB estimate of the local magnitude of the 16 August 1997 disturbance is  $M_L 3.8$ ; this is too low for the signals from the disturbance to be detected at most stations at teleseismic distances (between  $30^\circ$  and  $90^\circ$ ). At  $M_L 3.8$ , assuming the magnitude is reliable, it may be expected that the signals would be seen at mid-continental stations such as YKA in northern Canada. However, it has been shown from studies of the  $P$  signals from NNZ explosions that signals propagating north are reduced by attenuation such that the station magnitudes are about one magnitude unit less than the average (e.g., Marshall et al., 1994). It is thus no surprise that no signals from the 16 August 1997 disturbance have been observed at stations in North America.

All the stations reporting  $P$  from the 16 August disturbance lie at distances of less than  $22^\circ$  from the epicentre and the distribution of the stations with azimuth is poor; six of the detecting stations (in Scandinavia and western Russia) being confined to the azimuth range  $242^\circ$  to  $269^\circ$  (Figure 1b). Further, no surface waves are detected. Thus, none of the well established criteria for distinguishing between earthquakes and explosions, e.g., focal depth, relative sizes of body wave magnitude  $m_b$  and surface wave magnitude  $M_s$ , or radiation pattern can be applied. However, Marshall, Stewart and Lilwall (1989) have shown that the seismic disturbance of 1 August 1986 beneath the Kara Sea (Table 1) was an earthquake, principally on the basis of focal depth and radiation pattern; their epicentre is about 60 km from the REB epicentre for the 16 August 1997 disturbance. The source mechanism for the 1 August 1986 disturbance is an oblique reverse fault. The nodal planes for  $P$ ,  $SH$  and  $SV$  are shown in Figure 2.

The approach used for determining the most likely source mechanism for the 16 August 1997 disturbance is to compare the seismograms from the disturbance with those from NNZ explosions and from the 1 August 1986 earthquake. If the seismograms from the 16 August 1997 seismograms closely resemble those from the 1 August 1986 earthquake this will support the conclusion from the position of the epicentre that the 1997 disturbance is also an earthquake. If the seismograms from the NNZ explosions resemble those from the 16 August disturbance, this will support the claim that the 1997 disturbance was an explosion. However, if no resemblance is found then the 1997 disturbance cannot be identified using the available waveform data.

### 2.2 Available Waveform Data

Table 2 lists the stations recording seismograms that have been analysed from the 16 August 1997 disturbance. Four of the stations have good three-component recordings; the remainder of the recording stations are small aperture arrays, except for the large aperture array NORSAR. Figure 3 shows the vertical-component data used by the PIDC to locate the 16 August disturbance, the  $P$  arrival times reported in the REB are marked. The  $P$  waveforms at SPITS, FINES, HFS and NORES are the array beams calculated using the back-azimuth and phase velocity assuming the REB epicentre and the IASPEI 91 travel time tables (Kennett, 1991). Clearly, the  $P$  arrival times picked by the PIDC analysts are reasonable, although minor adjustments are probably desirable, these are of only a few seconds, indicating that the REB location is a fair estimate.

Figure 4 shows the  $S$  arrival times picked by the PIDC analysts, again SPITS and FINES are the array beam as above, but using the  $S$  phase velocity from the IASPEI 91 tables. The PIDC arrival

The large differences in the  $S/P$  ratios at KEV from the NNZ explosions and the 16 August 1997 disturbance suggest that if the epicentre of the 16 August disturbance is located at the NNZ test site, then the source is unlikely to be an explosion. Further, the large  $S/P$  ratios and impulsive nature of  $S$  on the T-component at KEV from the 16 August disturbance are features of synthetic seismograms calculated for an earthquake source in a Fennoscandian structure (Blandford, 1993). Figure 8 shows a comparison of the Z-component recorded at KAF from the 16 August disturbance and the NNZ explosion of 24 October 1990. Again the 16 August disturbance exhibits larger  $S/P$  ratios than the NNZ explosion. Unfortunately we have been unable to obtain data from KEV or KAF for the 1 August 1986 earthquake.

## 2.5 Discrimination Using $P$ Seismograms at NORSAR

NORSAR comprises 7 subarrays each of 6 seismometers within an aperture of about 10 km. The overall aperture is nearly 80 km (Figure 9). The small aperture NORES (NRA0) array lies within NORSAR. We were able to obtain data recorded at NORSAR from the 16 August 1997 disturbance, the Kara Sea earthquake of 1 August 1986 (Marshall et al., 1989), and a presumed NNZ explosion of 26 August 1984. We have formed beams on the centre element of each subarray. Table 3 summarises the results of the beamforming, and gives the location, epicentral distance and azimuth from the three disturbances to each subarray. Appendix A shows the individual waveforms and subarray beams summarised in Table 3. Clearly, the observed waveforms are, in general, incoherent between subarrays (many are incoherent within each subarray). The coherence of the  $P$  wavefield across each subarray can be quantified using semblance  $C$  which is similar to the mean correlation between subarray elements.  $C$  is defined as:

$$C = \frac{\sum_{k=1}^m \left( \sum_{i=1}^n s_i(k + t_i) \right)^2}{n \sum_{k=1}^m \sum_{i=1}^n s_i(k + t_i)^2},$$

where,  $n$  is the number of elements within the subarray,  $m$  is the number of samples,  $s_i(k)$  in the analysis window, and  $t_i$  is the time shift at the  $i^{\text{th}}$  element due to the apparent speed and azimuth of the  $P$  wavefield across the subarray.  $C$  is unity when the wavefield is perfectly correlated, and  $C=1/n$  for white Gaussian noise.

$C = \frac{1}{\Phi_{ds}^2}$ , where  $\Phi_{ds}$  is the noise reduction parameter of Douglas and Young (1981).

The first arrival 'A' was picked on the original seismogram recorded at the centre element of each subarray. If the centre element was not available then the time-shifted seismogram from the subarray element closest to the centre was used. The data are filtered with a passband of 0.8-4.5 Hz to remove low frequency noise before calculating  $C$  using four windows relative to 'A' defined as:

- 'noise': starts 2.5 seconds before 'A' and is 2.0 seconds long.
- '2 sec.': starts 0.1 seconds before 'A' and is 2.0 seconds long.
- '4 sec.': starts 0.5 seconds before 'A' and is 4.0 seconds long.
- 'coda': starts 3.5 seconds after 'A' and is 2.0 seconds long.

$S/P$  ratios to be robust, path and station corrections for each regional phase need to be calculated. These corrections are usually a complicated function of frequency.

Much of the research effort of the last 10 years has gone into generating synthetic regional distance seismograms in an attempt to reproduce  $S$  observed from explosions and earthquake sources, as this is the key to explaining why high frequency  $S/P$  ratios work as a discriminant. The models suggest that much of the observed  $S$  energy does not originate from a simple point explosion source, but may be caused by the spalling of above-source material. This spall is represented in some models as the opening and closing of a horizontal crack, and in others as a compensated linear vector dipole (CLVD).  $S$  is produced by the horizontal crack and CLVD models, but the CLVD representation also relies on near-source scattering of  $R_g$ -to- $S$  energy. Another source of high frequency  $S$  energy from explosions is from small cracks in the volume of rock surrounding the explosion source. This may also be the explanation of high frequency  $S$  from earthquakes.

Neither of the spall representations directly produce  $SH$  energy, so if spall is the source of high frequency  $S$  from explosions then  $S$  energy observed on the tangential component must be scattered (Gupta and Blandford, 1983). Experiments show that  $S/P$  ratios are higher for well-contained explosions than for decoupled explosions, suggesting that at least some  $S$  energy originates from small cracks surrounding the explosion source. The  $S$  energy from small cracks surrounding the explosion may have a significant  $SH$  component depending on the orientation of the cracks, but this may not be detected if there is sufficient scattering.

Blandford (1993) calculated synthetic seismograms for a Fennoscandian structure and showed that while some earthquake mechanisms have explosion-like  $S/P$  ratios estimated from the vertical component, the same mechanisms produce large (earthquake-like)  $S/P$  ratios on the tangential component. Further, modelling suggests that well-contained explosions would be expected to show more emergent  $S$  arrivals than earthquakes or explosions with significant spall. It should be noted that the separation between high frequency  $S/P$  earthquake and explosion populations predicted by the synthetic seismograms is almost always greater than that observed. However, the studies using synthetic seismograms show that there is a physical basis for discrimination using  $S/P$  ratios.

Here we use an empirical approach and examine  $S/P$  ratios from waveforms recorded at KAF and KEV from the 16 August 1997 disturbance and NNZ explosions. We hope to answer the question, 'are the  $S/P$  ratios observed from the 16 August disturbance consistent with an explosion at the NNZ test site?'

## 2.4 Applying $S/P$ Ratios as a Discriminant

Figures 7a-d show three-component waveforms rotated into the Z, R and T components from four NNZ explosions (Table 1) recorded at KEV. The data are filtered with a passband of 3.0-6.0 Hz so a direct comparison can be made with the three-component seismograms at KEV from the 16 August 1997 disturbance (Figure 6c). The  $P$  and  $S$  times are calculated using the IASPEI 91 tables and the epicentres and origin times shown in Table 1. The observations in Figure 7 show good repeatability between explosions. The  $S/P$  ratio on the Z-component is much less than unity, whereas the  $S/P$  ratio on the R and T components is about unity. Clearly, the  $S/P$  ratios observed from the NNZ explosions are much lower than those in Figure 6c from the 16 August disturbance. Also,  $S$  on the T-component from the explosions appears more emergent than that from the 16 August 1997 disturbance.

al. (1989) determined the maximum likelihood estimate of  $m_b$  for the 1 August 1986 earthquake to be 4.26, we can thus estimate  $m_b$  for the 16 August 1997 disturbance.

In the previous section we showed that only NAO and NC4 have reasonably coherent subarray beams from both the 16 August 1997 and 1 August 1986 disturbances (Table 4). The amplitude ratio of  $P$  from the two disturbances at NAO is about 8, while that for NC4 is about 11. This suggests that the maximum likelihood estimate of  $m_b$  for the 16 August 1997 disturbance is between 3.22 and 3.36.

### 3. DISCUSSION

Figure 3 shows that  $P$  observed at HFS and NORES has a large amplitude, appears 'simple' comprising a single impulsive arrival with apparent positive (compressional) first motion and small amplitude coda, and contains high frequencies (above the noise at least up to 8 Hz). All these waveform features are similar to those seen on seismograms from well-contained NNZ explosions recorded at NORES. However, they do not necessarily mean that the disturbance producing these waveform features is an explosion. There are certain earthquake orientations that result in 'simple' seismograms (Bowers, 1996), positive first motions are commonly observed from reverse-type earthquake mechanisms, and earthquakes at crustal depths commonly generate significant high frequency energy.

It is interesting to note from the lower hemisphere focal projections in Figure 2 that NORES and HFS would plot just below the 'T' showing the position of the tension axis, or maximum of the earthquake radiation pattern, for the fault plane solution of Marshall et al. (1989) for the 1 August 1986 Kara Sea earthquake. Downward  $P$  to NORES from this earthquake mechanism would have positive polarity. Also the surface reflections  $pP$  and  $sP$  are near minima in their respective radiation patterns, and any above-source structure will further reduce the amplitude of  $pP$  and  $sP$ . Thus the  $P$  seismogram at NORES would be expected to appear 'simple'. So explosion-like observations at HFS and NORES from the 16 August disturbance can also be explained by an earthquake with a similar mechanism to that determined by Marshall et al. (1989) for the 1 August 1986 Kara Sea earthquake.

Marshall et al. (1989), referring to the 1 August 1986 earthquake, stated that 'if the magnitude of this particular source had been a little lower it may not have been possible to identify...'. Indeed it has only been possible to identify the 16 August 1997 disturbance as an earthquake because of: (1) good azimuthal coverage of stations resulting in small uncertainties in the longitude of the epicentre, and (2) archived waveform data (at KEV, KAF and NORSAR) enabling a direct comparison to be made between waveforms from the 16 August disturbance and previously identified explosions and an earthquake. This clearly demonstrates that archived waveform data from previously identified disturbances is an invaluable resource if attempting to identify small seismic disturbances close to the detection threshold. Further, it demonstrates that whereas new stations are useful at improving location accuracy, it is stations with archived waveform data that are crucial to effective discrimination close to the detection threshold where empirical methods have to be employed. Obviously, for stations with archived waveform data to be useful in monitoring the Comprehensive Test Ban Treaty (CTBT) they have to continue to operate along with new stations.



The results are shown in Table 4 for subarrays with 3 or more elements. The 'reasonably coherent beam' in Table 3 is arbitrarily defined as a subarray with semblance  $C \geq 0.45$ , where  $C$  is calculated using the '2 sec.' window defined above. The 'NORSAR' row in Table 4 shows semblance values calculated using the subarray beams, these clearly demonstrate that subarrays within NORSAR are incoherent.

There is great variation in the waveforms and associated semblance values observed across NORSAR, which have been attributed to complex upper mantle structure, the structure of the Oslo Graben, and the large variations in topography. Figures 10a-e compare the subarray beams from the three disturbances. However, consideration of the signal-to-noise ratio and the semblance values (Table 4) suggest that only the subarray beams at NAO (Figure 10a), NC4 (Figure 10e), and perhaps NB2, offer a meaningful comparison.

At far-regional distances of about  $21^\circ$  observed  $P$  typically has a series of phases arriving within the first few seconds, these 'triplications' are notoriously difficult to interpret. Ringdal (1980) reports  $P$  arrivals at NORSAR at similar distances from a series of North Caspian Sea explosions, and shows that the form of the  $P$  waveform is highly sensitive to epicentral distance.

Given the general incoherence of  $P$  observed at the NORSAR subarrays (Table 4), the similarity of the 16 August 1997 and 1 August 1986 subarray beams at NAO and NC4 in Figure 10 is remarkable. This suggests that  $P$  from the two disturbances travelled similar paths to each subarray, and that the two disturbances are at similar epicentral distances. Further, since the 1 August disturbance has been identified as an earthquake by Marshall et al. (1989), the similarity of the waveforms at NAO and NC4 indicates that the 16 August disturbance is also an earthquake, possibly with a similar mechanism. The different character of  $P$  at NAO and NC4 from the presumed NNZ explosion of 26 August 1984 suggests that it travels a different path to  $P$  from the 1 August and 16 August disturbances, and that it is located at a different epicentral distance.

Marshall et al. (1989) calculated the epicentre of the 1 August 1986 Kara Sea earthquake (Table 1) using  $P$  travel time corrections derived from JED locations of NNZ explosions (Lilwall and Marshall, 1986). Table 1 show the results of the JED for the 16 August 1997 disturbance calculated using five NNZ explosions and  $P$  arrival times from 8 regional stations (R.G. North, written communication). Figure 11 compares the JED locations for the 1 August and 16 August disturbances, also shown is the 90% confidence ellipse for the 16 August disturbance determined by R.G. North (written communication) with major axis 70.7 km, minor axis 8.0 km, and bearing  $354.2^\circ$ . Clearly the JED solutions suggest that the 1 August and 16 August disturbances are almost co-located, as inferred from the comparison of the NORSAR subarray beams.

## 2.6 Estimates of the Body Wave Magnitude

The NORSAR array estimate of the body wave magnitude by F. Ringdal (written communication) is 3.39  $m_b$ , and that by the Center for Monitoring Research is 3.68 (R.G. North, written communication). Since  $m_b$  from small disturbances is inevitably biased high we use an alternative method using the subarray beams at NORSAR.

NORSAR recorded waveforms from both the 16 August 1997 disturbance and the 1 August 1986 Kara Sea earthquake. Since the two disturbances are at nearly the same epicentral distance from each NORSAR subarray (Table 3), the ratio of the amplitudes from the two disturbances at each subarray will give an estimate of the relative size of the disturbances. Further, since Marshall et

## REFERENCES

- Blandford, R.R., 1993. Discrimination of earthquakes and explosions at regional distances using complexity. AFTAC-TR-93-044, HQ AFTAC, Patrick AFB, FA, USA.
- Blandford, R.R., 1996. Regional seismic event discrimination. In 'Monitoring a Comprehensive Test Ban Treaty', E.S. Husebye and A.M. Dainty (eds), pp689-719.
- Bowers, D., 1996. On the probability of mistaking an earthquake for an explosion using the simplicity of  $P$ . *Bull. Seis. Soc. Am.*, **86**, 1925-1934.
- Douglas, A. and Young, J.Y., 1981. The estimation of seismic body wave signals in the presence of oceanic microseisms. AWRE Report No. O 14/81, HMSO, London.
- Fisk, M.D., 1997. Event characterization analysis of the 16 August 1997 event in the Kara Sea. Draft Technical Report, Mission Research Corporation, Newington, VA, USA.
- Frohlich, C., 1996. Cliff's nodes concerning plotting nodal lines for  $P$ ,  $SH$  and  $SV$ . *Seis. Res. Lett.*, **67**, 16-24.
- Gupta, I.N. and Blandford, R.R., 1983. A mechanism for generation of short period transverse motions from explosions. *Bull. Seis. Soc. Am.*, **73**, 571-592.
- Kennett, B.L.N., 1991. IASPEI 1991 Seismological Tables. Research School of Earth Sciences, Australian National Univ., Canberra, Australia.
- Lilwall, R.C. and Marshall, P.D., 1986. Body wave magnitudes and locations of Soviet underground explosions at the Novaya Zemlya test site. AWRE Report No. O 17/86, HMSO, London.
- Marshall, P.D., Stewart, R.C. and Lilwall, R.C., 1989. The seismic disturbance on 1986 August 1 near Novaya Zemlya: a source of concern? *Geophys. J.*, **98**, 565-573.
- Marshall, P.D., Porter, D., Young, J.B. and Peachell, P.A., 1994. Analysis of short-period seismograms from explosions at the Novaya Zemlya test site in Russia. AWE Report No. O 2/94, HMSO, London.
- Richards, P.G. and Kim, W.Y., 1997. Testing the nuclear test ban treaty. *Nature*, **389**, 781-782.
- Ringdal, F., 1981. Location of regional events using travel time differentials between  $P$  arrival branches. NORSAR Sci. Rep. No. 2 1980/81, NTNF/NORSAR, Kjeller, Norway.
- Ryall, A.S., Baumgardt, D.R., Fisk, M.D. and Riviere-Barbier, F., 1996. Resolving regional discrimination problems: some case histories. In 'Monitoring a Comprehensive Test Ban Treaty', E.S. Husebye and A.M. Dainty (eds), pp721-741.
- van der Vink, G.E. and Wallace, T.C., 1996. The political sensitivity of earthquake locations. IRIS Newsletter, **15**, No. 3, pp20-23.

#### 4. CONCLUSIONS

From our analysis of the available seismic waveform data from the 16 August 1997 disturbance and from an earthquake and several explosions in the Novaya Zemlya region we reach the following conclusions.

- i) Examination of the arrival times in the REB suggests that the PIDC location for the 16 August disturbance is reasonable.
- ii) From consideration of the azimuthal distribution of the three closest stations (KEV, NRI, and SPITS) it is difficult to see how the epicentre of the 16 August disturbance can be anywhere other than in the Kara Sea.
- iii) The  $S/P$  ratios observed at KEV and KAF from the 16 August disturbance are different from those observed from NNZ explosions. Further, the observed  $S/P$  ratios and comparatively impulsive  $S$  onset on the tangential component at KEV from the 16 August 1997 disturbance are similar to those predicted for earthquakes using recent modelling techniques.
- iv) A comparison of  $P$  at NORSAR subarrays NAO and NC4 suggests that the 16 August 1997 disturbance has a similar location and mechanism to the 1 August 1986 Kara Sea earthquake.
- v) A comparison of JED epicentres from the 1 August 1986 earthquake and the 16 August 1997 disturbance also suggests they are nearly co-located.
- vi) Consideration of the radiation pattern from the 1 August 1986 Kara Sea earthquake suggests that such a mechanism would result in 'simple' seismograms being observed at NORES and HFS, with positive (compressional) first motion.
- vii)  $P$  from NORSAR suggests that the maximum likelihood estimate of  $m_b$  for the 16 August 1997 disturbance is about 3.3.

#### 5. ACKNOWLEDGMENTS

We thank Matti Tarvainen (University of Helsinki) and Svein Mykkeltveit (NORSAR) for providing seismograms. IRIS provided the KEV seismograms from four NNZ explosions. The PIDC provided the REB and other waveform data. The GMT mapping package (Wessel and Smith, 1991) was used to prepare Figures 1a, 1b, and 11. Cliff Frohlich's 'nodes' program (Frohlich, 1996) was used to prepare Figure 2.

**Table 1**

**Source Parameters of Novaya Zemlya Disturbances**

<b>Date</b>	<b>Origin Time (UTC)</b>	<b>Lat (°N)</b>	<b>Long (°E)</b>	<b>Depth (km)</b>	<b>m<sub>b</sub></b>	<b>Reference</b>
16 August 1997	02-10-59.9	72.648	57.352	0	3.9	REB
	02-10-59.7	72.835	57.225	10	3.2	PDE
	02-11-02.1	72.991	56.942	0	3.68	JED, R.G. North (written communication)
<b>Earthquakes</b>						
1 August 1986	13-56-37.8	73.031	56.726	24 <sup>†</sup>	4.26	Marshall et al. (1989)
<b>Explosions</b>						
26 August 1984	03-30-00.0	74	54	-	4.2	NORSAR monthly bulletin
2 August 1987	02-00-00.2	73.326	54.611	0	5.82	Marshall et al. (1994)
7 May 1988	22-49-58.3	73.314	54.562	0	5.58	Marshall et al. (1994)
4 December 1988	05-19-53.3	73.366	55.010	0	5.89	Marshall et al. (1994)
24 October 1990	14-57-58.5	73.331	54.766	0	5.6 <sup>‡</sup>	Marshall et al. (1994)

<sup>†</sup> Model II: Strike: 253°, Dip Angle: 130°, Slip Angle: 147°

<sup>‡</sup> From NORSAR Sci. Rep. No. 2 - 90/91.

Walter, W.R., Mayeda, K.M. and Patton, H.J., 1995. Phase and spectral ratio discrimination between NTS earthquakes and explosions. Part 1: empirical observations. *Bull. Seis. Soc. Am.*, **85**, 1050-1067.

Wessel, P. and Smith, W.H.F., 1991. Free software helps map and display data. *EosTrans, AGU*, **72**, 441, 445-446.

#### **NOTE ADDED IN PROOF**

During publication of this report the following relevant articles have appeared in the literature:

- i) Review by R.J. Smith in the Washington Post (20 October 1997) gives background information, and describes the interaction of the science and politics related to the 16 August disturbance..
- ii) Richards and Kim (1997) identify the 16 August 1997 disturbance as an earthquake on the basis of its location and vertical component *S/P* ratios at KEV compared with those from underground explosions at NNZ.
- iii) Fisk (1997) suggests that the waveform data from the 16 August 1997 disturbance are consistent with an earthquake in the Kara Sea, but are inconsistent with an underground explosion at NNZ.
- iv) On the 4 November 1997 the Washington Post reported 'U.S. formally drops claim of possible nuclear blast'.

**Table 3**  
**NORSAR Subarrays**

Subarray Code	Location of Centre Element		16 August 1997 (REB epicentre)				1 August 1986				26 August 1984			
	Lat (°N)	Long(°E)	Δ(°)	Az(°)	BQ*	No. of Stns used	Δ(°)	Az(°)	BQ*	No. of Stns used	Δ(°)	Az(°)	BQ*	No. of Stns used
NAO	60.82372	10.83236	21.1	260	✓	5	21.0	259	✓	4	20.5	253	x	5
NBO	61.03075	10.77739	21.0	261	x	2	20.9	259	✓	6	20.3	254	✓	6
NB2	61.03972	11.21475	20.9	260	✓	6	20.7	259	✓	6	20.2	253	✓	5
NC2	61.28067	10.83539	20.8	261	✓	3	-	-	-	-	20.1	254	✓	6
NC3	61.26170	11.41414	20.6	261	x	6	20.5	259	x	4	20.0	253	x	6
NC4	61.07906	11.71886	20.7	260	✓	6	20.6	258	✓	6	20.1	253	✓	6
NC6	60.74731	11.45839	21.0	260	x	5	20.9	258	x	5	-	-	-	-

\*BQ - subarray beam quality

✓ = reasonably coherent beam ( $C \geq 0.45$ , '2 sec.' window)

x = incoherent beam ( $C < 0.45$ , '2 sec' window)

- = data not available/usable

**Table 2**

**Seismograms analysed for the 16 August disturbance<sup>1</sup>**

	Station	Distance <sup>2</sup> (°)	Azimuth <sup>2</sup> (°)	Type of Station	Data Presented in this Report	
					1 August 1986	NNZ Explosion(s)
	APA, Apatity, RF	9.59	249.8	Array 2 km aperture	No	No
	KEV, Kevo, Finland	10.13	268.3	3 cpt station	No	Yes
	NRI, Norilsk, RF	10.62	94.9	Vertical cpt station	No	No
	SPA0, SPITS, Spitsbergen	11.44	317.0	Array 2 km aperture	No	No
14	KAF, Kajaani, Finland	15.68	243.8	3 cpt station	No	Yes
	FIA0, FINESA, Finland	16.30	242.7	Array 2 km aperture	No	No
	HFS, Hagfors, Sweden	20.85	256.1	Array 2 km aperture	No	No
	NRA0, NORES, Norway	21.00	259.5	Array 2 km aperture	No	No
	NAO, NORSAR, Norway	21.14	260.4	Large aperture array	Yes	Yes

<sup>1</sup>ARCES in northern Norway was out of operation. Seismograms from ARU, ATUK, EKA, PDY, YKA and ZAL were also inspected but no signals were seen.

<sup>2</sup>Measured from the epicentre published in the REB: 72.648°N, 57.352°E.

## Figure Captions

- Figure 1 (a) Azimuthal equidistant projection, centred on the North Novaya Zemlya test site (NNZ), showing the epicentre of the 1 August 1986, Kara Sea earthquake, and the REB and PDE epicentre of the 16 August 1997 disturbance. (b) Azimuthal equidistant projection centred on NNZ showing the location of stations (listed in Table 2) recording seismic signals from the 16 August 1997 disturbance.
- Figure 2 Lower hemisphere equal area stereographic projections showing the nodal planes of  $P$ ,  $SH$  and  $SV$ , for the mechanism (Model II) determined by Marshall et al. (1989) for the 1 August 1986 Kara Sea earthquake. T, B and P mark the axes of maximum, intermediate and minimum moment. T corresponds to the maximum positive (compressive) polarity and P the maximum negative (dilatational) polarity of the earthquake  $P$ -radiation. B is the null axis.
- Figure 3 Vertical-component  $P$  waveforms from stations reporting in the REB for the 16 August 1997 disturbance. 'P' marks the onset time picked by the PIDC analysts.
- Figure 4 Vertical-component  $S$  waveforms from stations reporting in the REB for the 16 August 1997 disturbance. 'S' marks the onset time picked by the PIDC analysts.
- Figure 5 Vertical-component seismograms from 8 stations recording  $P$  from the 16 August 1997 disturbance. The waveforms are aligned on the  $P$  arrival time (Pi91) predicted using the REB location and origin time and the IASPEI 91 tables. All waveforms except those at HFS and NORES have been filtered with a passband of 3.0-6.0 Hz. SPITS, FINES, HFS and NORES are array beams. ' $P_{NZ}$ ' marks the onset, predicted using the IASPEI 91 tables, from a hypothetical disturbance at NNZ with origin time 02:11:05.0 UTC.
- Figure 6 Three-component seismograms recorded at FIA0, KAF, KEV and SPITS from the 16 August 1997 disturbance. The components have been rotated to the ray-coordinate directions of vertical (upper trace), radial (middle trace) and tangential (lower trace). The  $P$  (Pi91) and  $S$  (Si91) arrival times predicted using the IASPEI 91 tables and the REB location and origin time are marked. (a) FIA0 filtered with a passband of 2.0-4.0 Hz, (b) KAF filtered with a passband of 2.0-4.0 Hz, (c) KEV filtered with a passband of 3.0-6.0 Hz, and (d) SPB4 filtered with a passband 3.0-6.0 Hz.
- Figure 7 Three-component seismograms from four NNZ explosions recorded at KEV filtered with a passband of 3.0-6.0 Hz. The components are rotated as described in Figure 6. Pi91 and Si91 are calculated using the origin and location given in Table 1 and the IASPEI 91 tables. (a) 2 August 1987, (b) 7 May 1988, (c) 4 December 1988, and (d) 24 October 1990.
- Figure 8 Vertical-component seismograms recorded at KAF from the 16 August 1997 disturbance (upper trace), and the NNZ explosion of 24 October 1990 (lower trace). The data are filtered with a passband of 3.0-6.0 Hz. Pi91 and Si91 are calculated as in Figure 7.



**Table 4**

**Semblance Values at NORSAR**

	16 August 1997					1 August 1986					26 August 1984				
	1/n	noise	2 sec.	4 sec.	coda	1/n	noise	2 sec.	4 sec.	coda	1/n	noise	2 sec.	4 sec.	coda
NAO	0.20	0.10	0.67	0.56	0.16	0.25	0.33	0.80	0.73	0.50	0.20	0.09	0.35	0.32	0.33
NBO	-	-	-	-	-	0.17	0.08	0.78	0.73	0.65	0.17	0.19	0.54	0.66	0.55
NB2	0.17	0.13	0.45	0.39	0.45	0.17	0.14	0.73	0.71	0.43	0.20	0.14	0.47	0.55	0.43
NC2	0.33	0.51	0.72	0.64	0.41	-	-	-	-	-	0.17	0.22	0.60	0.74	0.63
NC3	0.17	0.09	0.26	0.27	0.28	0.25	0.34	0.34	0.68	0.65	0.17	0.11	0.23	0.44	0.54
NC4	0.17	0.12	0.53	0.47	0.20	0.17	0.29	0.61	0.59	0.65	0.17	0.10	0.49	0.64	0.61
NC6	0.20	0.15	0.32	0.34	0.32	0.20	0.08	0.42	0.50	0.49	-	-	-	-	-
NORSAR		0.18	0.18	0.21	0.26		0.09	0.26	0.33	0.12		0.25	0.13	0.43	0.26

n = number of elements in each subarray.  
 1/n = theoretical semblance value for white Gaussian noise.  
 'A' = *P* onset.

noise = semblance calculated using a 2.0 second long window starting 2.5 seconds before 'A'.  
 2 sec. = semblance calculated using a 2.0 second long window starting 0.1 seconds before 'A'.  
 4 sec. = semblance calculated using a 4.0 second long window starting 0.5 seconds before 'A'.  
 coda = semblance calculated using a 2.0 second long window starting 3.5 seconds after 'A'.

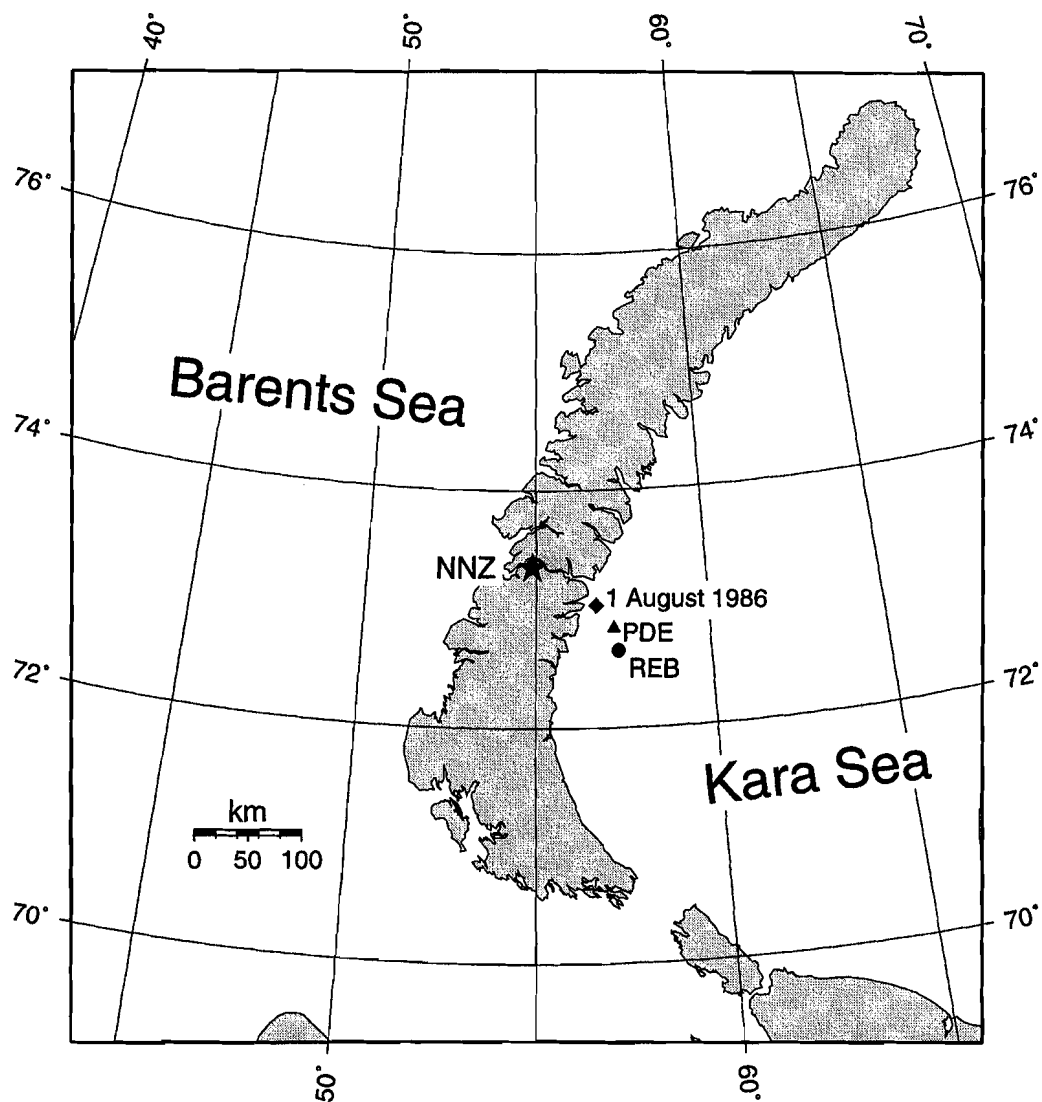


Figure 1a: Azimuthal equidistant projection, centred on the North Novaya Zemlya test site (NNZ), showing the epicentre of the 1 August 1986 Kara Sea earthquake, and the REB and PDE estimates of the 16 August 1997 epicentre.

- Figure 9 Map showing the location of the subarrays in the large aperture array NORSAR. The triangle indicates the location of the small aperture array NORES (NRA0).
- Figure 10 Comparison of the NORSAR subarray *P* beams. The upper trace is from the 16 August 1997 disturbance, the middle trace is from the 1 August 1986 Kara Sea earthquake, and the lower trace is from a presumed NNZ explosion on 26 August 1984 for subarrays (a) NAO, (b) NBO, (c) NB2, (d) NC3, and (e) NC4.
- Figure 11 Azimuthal equidistant projection centred on NNZ (star), showing the epicentre of the 1 August 1986 Kara Sea earthquake determined by Marshall et al. (1989) (diamond), and the JED epicentre of the 16 August 1997 disturbance determined by R.G. North (written communication) (circle). The 90% confidence ellipse for the 16 August JED epicentre is also shown.

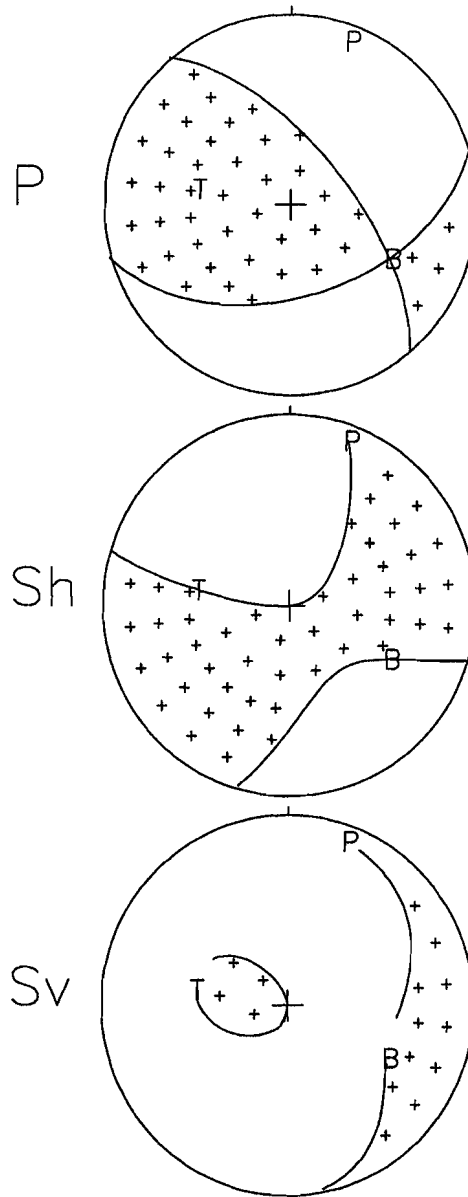


Figure 2: Lower hemisphere equal area projection showing the nodal planes of  $P$ ,  $SH$  and  $SV$ , for the mechanism (Model II) determined by Marshall et al. (1989) for the 1 August 1986 Kara Sea earthquake. T, B and P mark the axes of maximum, intermediate and minimum moment. T corresponds to the maximum positive (compressional) polarity and P the maximum negative (dilatational) polarity of the earthquake  $P$ -radiation. B is the null axis.

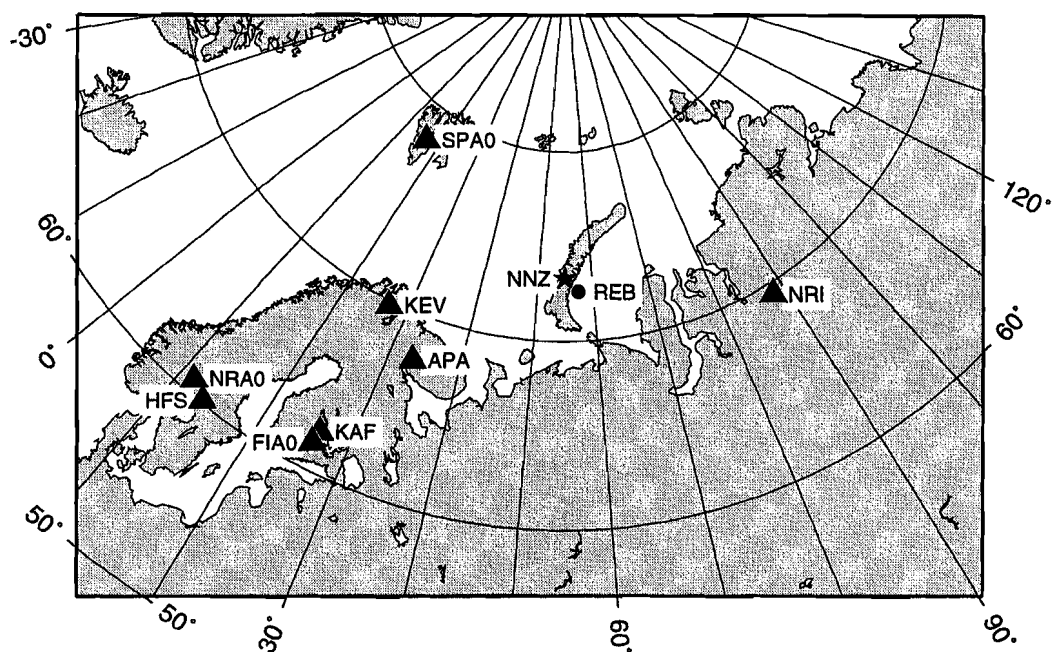


Figure 1b: Azimuthal equidistant projection centred on NNZ showing the location of stations (listed in Table 2) recording seismic signals from the 16 August 1997 disturbance.

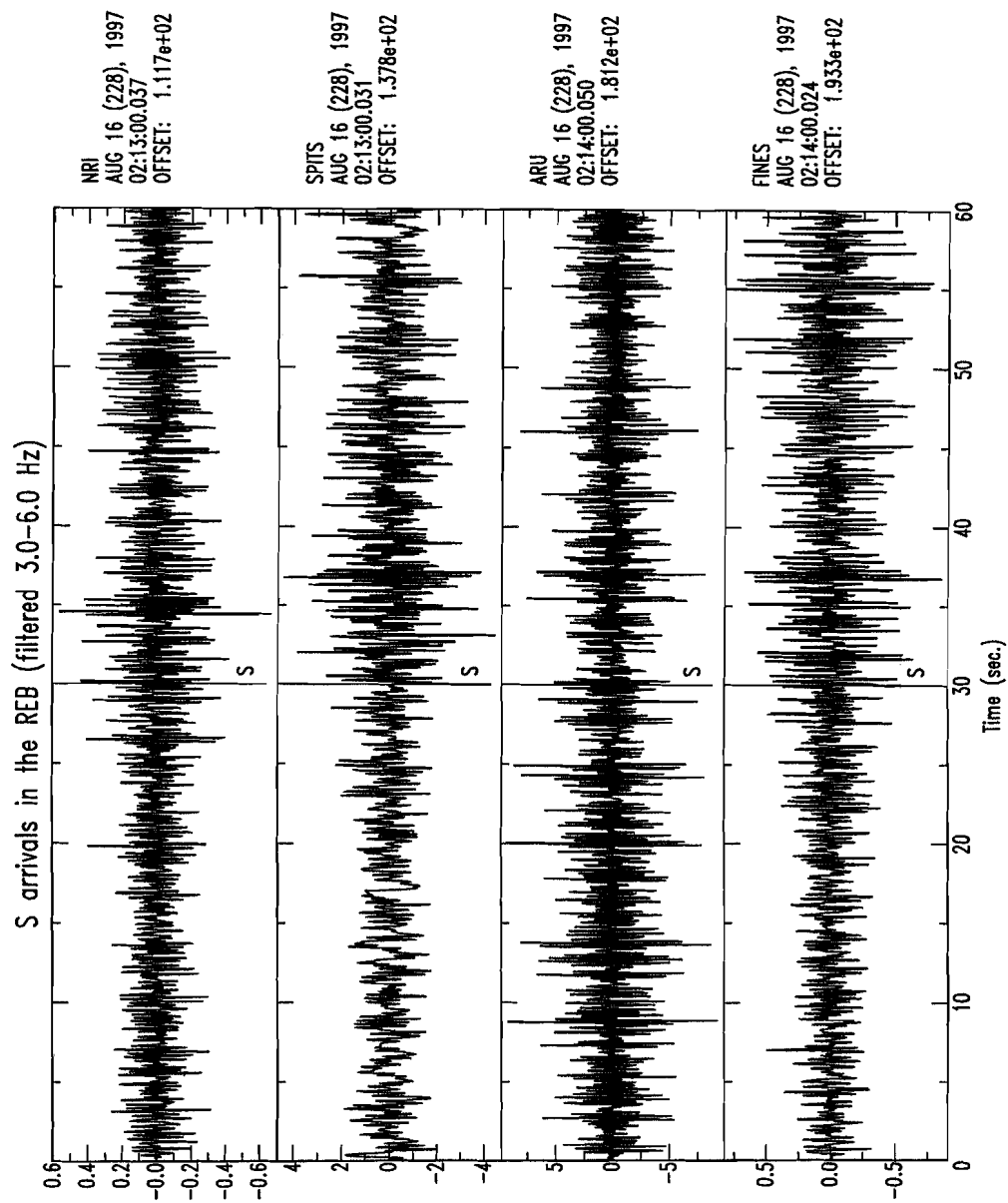


Figure 4: Vertical-component *S* waveforms from stations reporting in the REB for the 16 August 1997 disturbance. 'S' marks the onset time picked by the PIDC analysts.

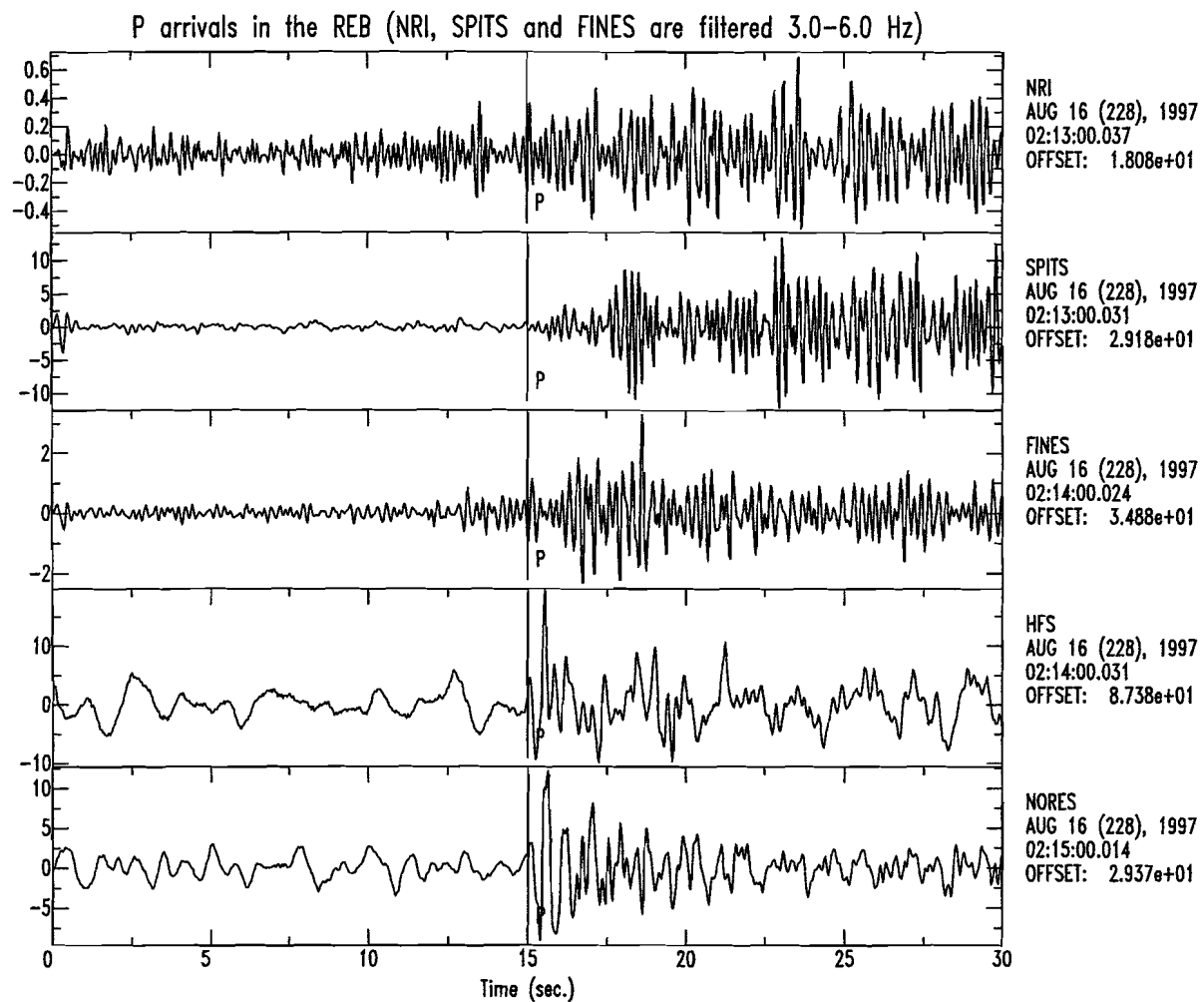


Figure 3: Vertical-component *P* waveforms from stations reporting in the REB for the 16 August 1997 disturbance. 'P' marks the onset time picked by the PIDC analysts.

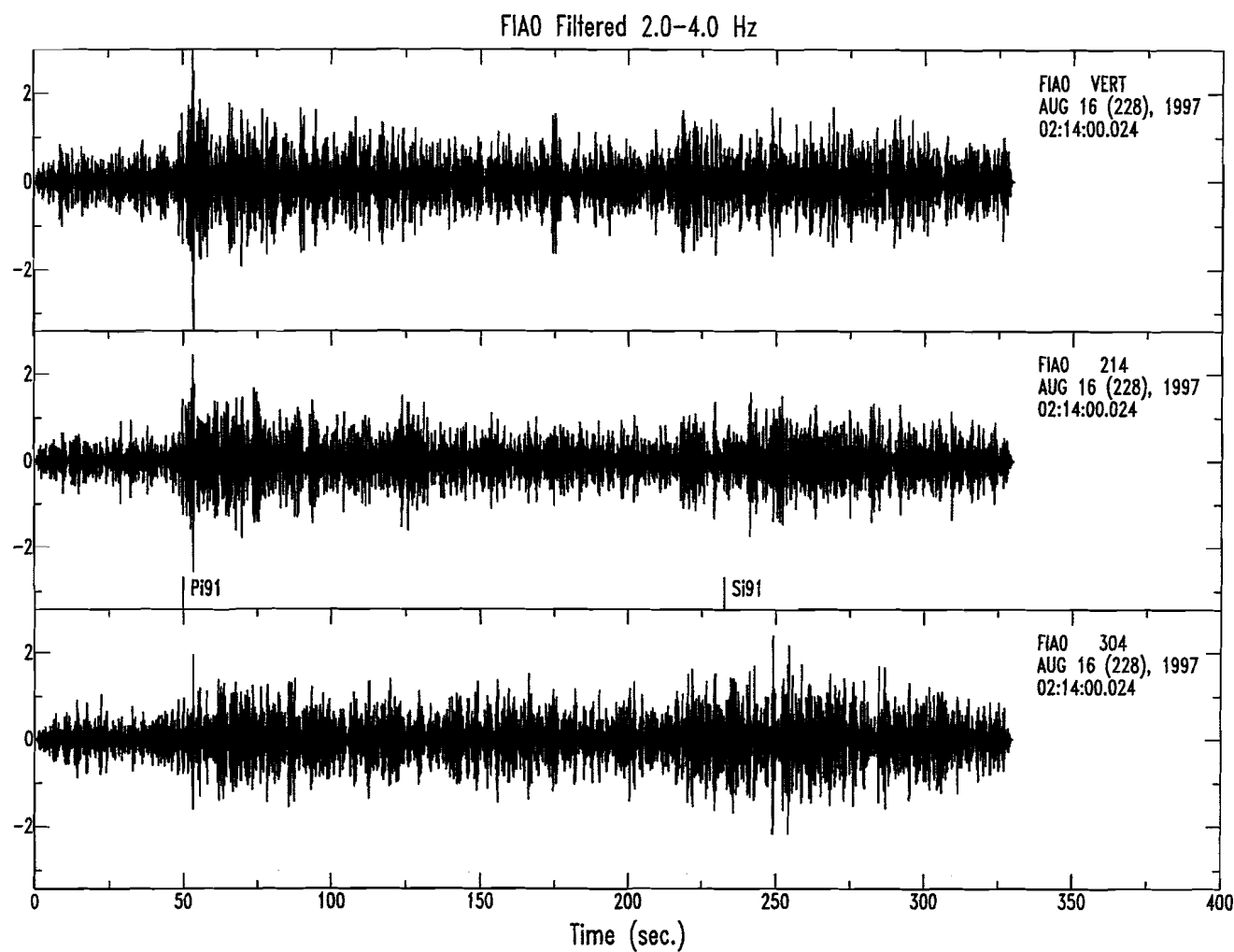


Figure 6a: Three-component seismograms recorded at FIA0 from the 16 August 1997 disturbance. The components have been rotated to the ray-coordinate directions of vertical (upper trace), radial (middle trace), and tangential (lower trace). The *P* (Pi91) and *S* (Si91) arrival times predicted using the IASPEI 91 tables and the REB location and origin time are marked. The data have been filtered with a passband of 2.0-4.0 Hz.



# P predicted from REB epicentre using IASPEI 91

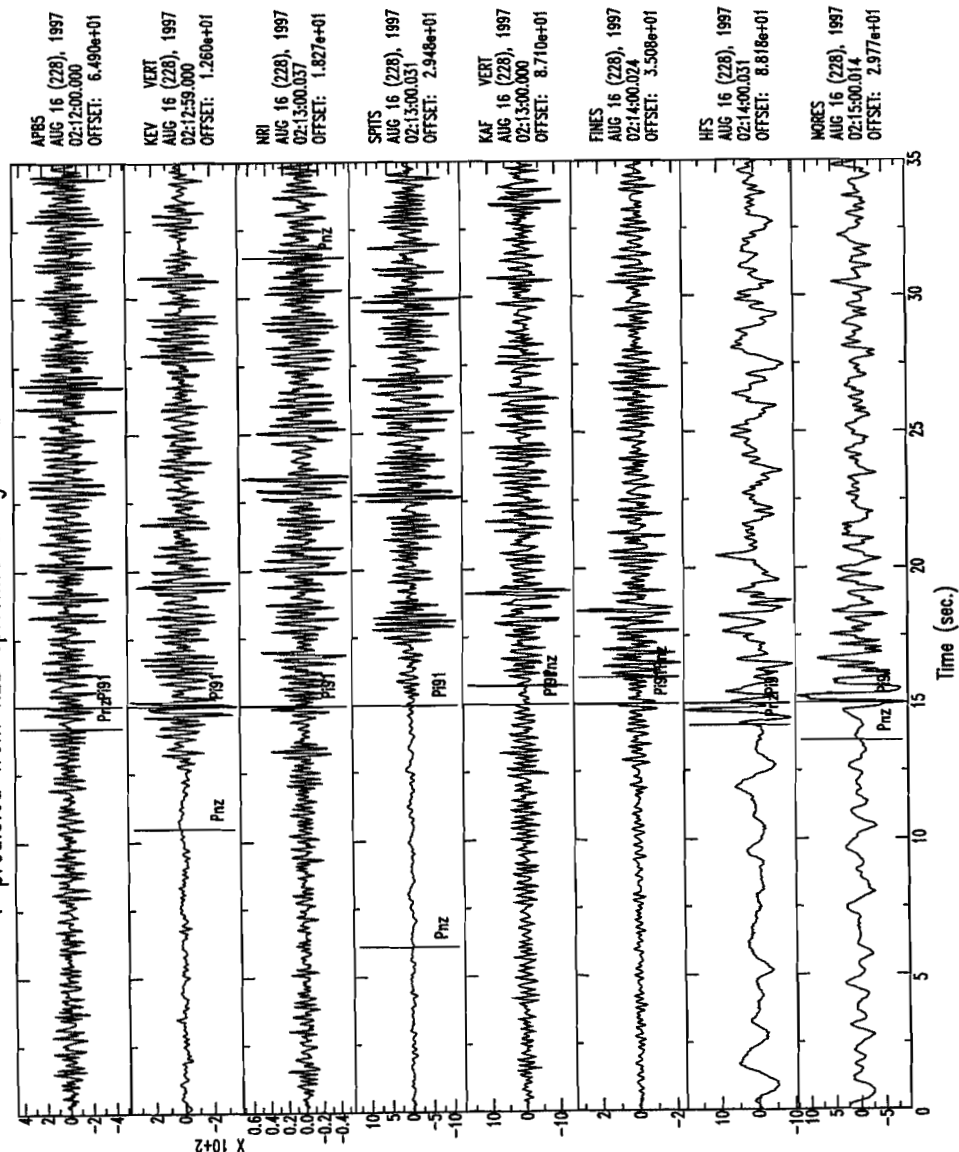


Figure 5: Vertical-component seismograms from 8 stations recording *P* from the 16 August 1997 disturbance. The waveforms are aligned on the *P* arrival time (Pi91) predicted using the REB location and origin time and the IASPEI 91 tables. All waveforms except those at HFS and NORES have been filtered with a passband of 3.0-6.0 Hz. SPITS, FINES, HFS, and NORES are array beams. 'Pnz' marks the onset predicted using the IASPEI 91 tables from a hypothetical disturbance at NNZ with origin time 02:11:05.0 UTC.

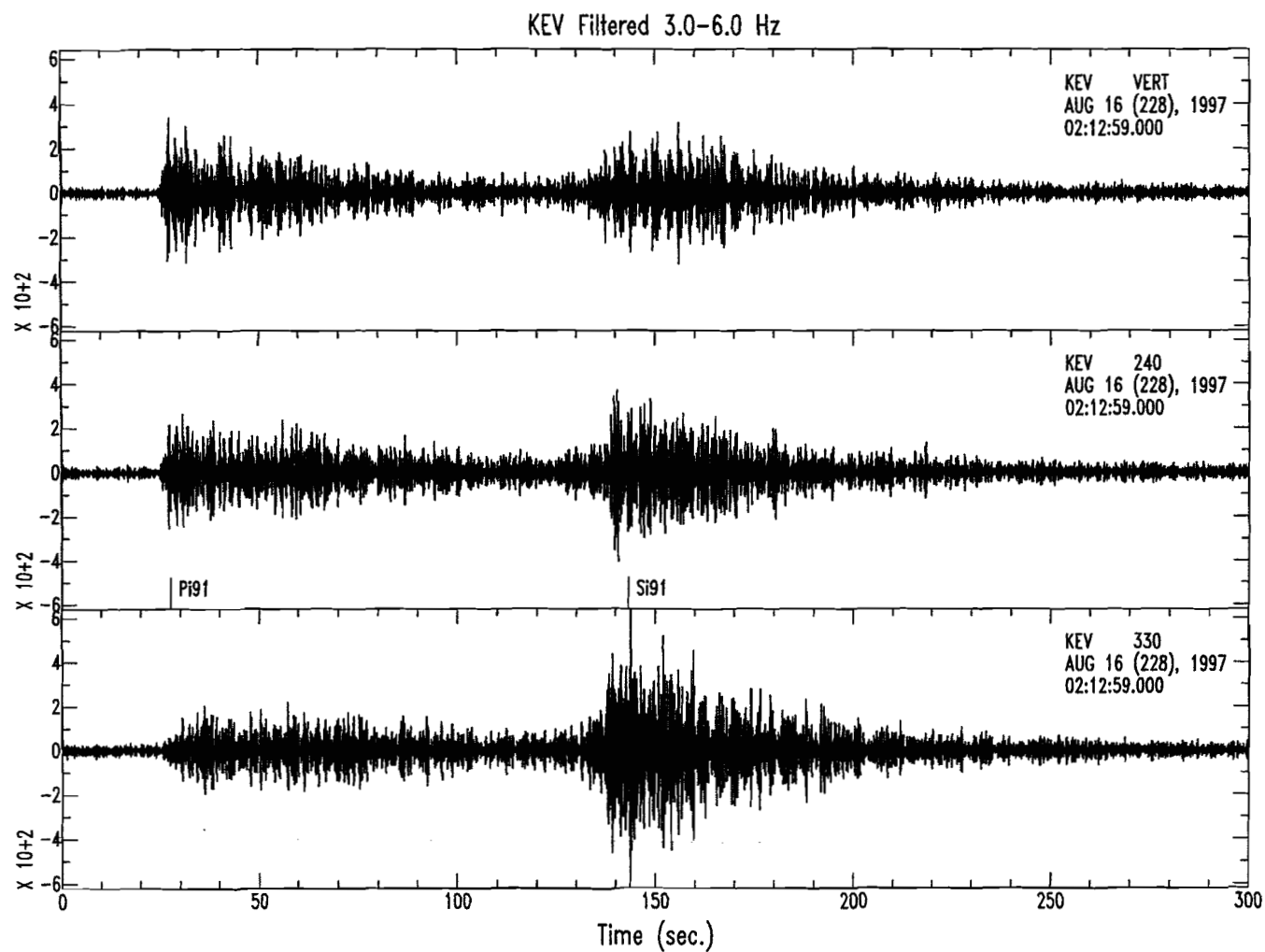


Figure 6c: Three-component seismograms recorded at KEV from the 16 August 1997 disturbance. The components are rotated as described in Figure 6a. Pi91 and Si91 are also as described in Figure 6a. The data have been filtered with a passband of 3.0-6.0 Hz.

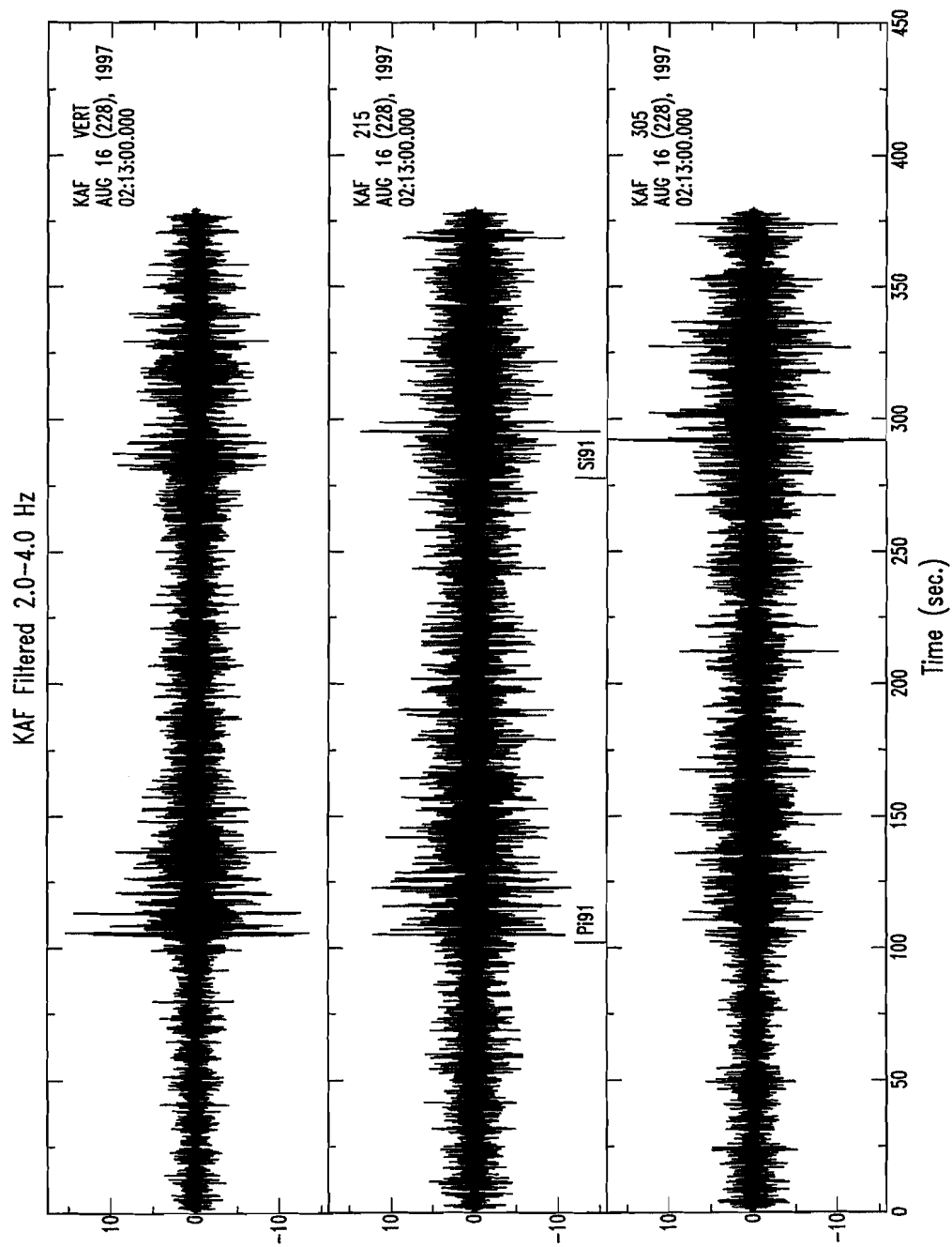


Figure 6b: Three-component seismograms recorded at KAF from the 16 August 1997 disturbance. The components are rotated as described in Figure 6a. Pi91 and Si91 are also as described in Figure 6a. The data have been filtered with a passband of 2.0-4.0 Hz.

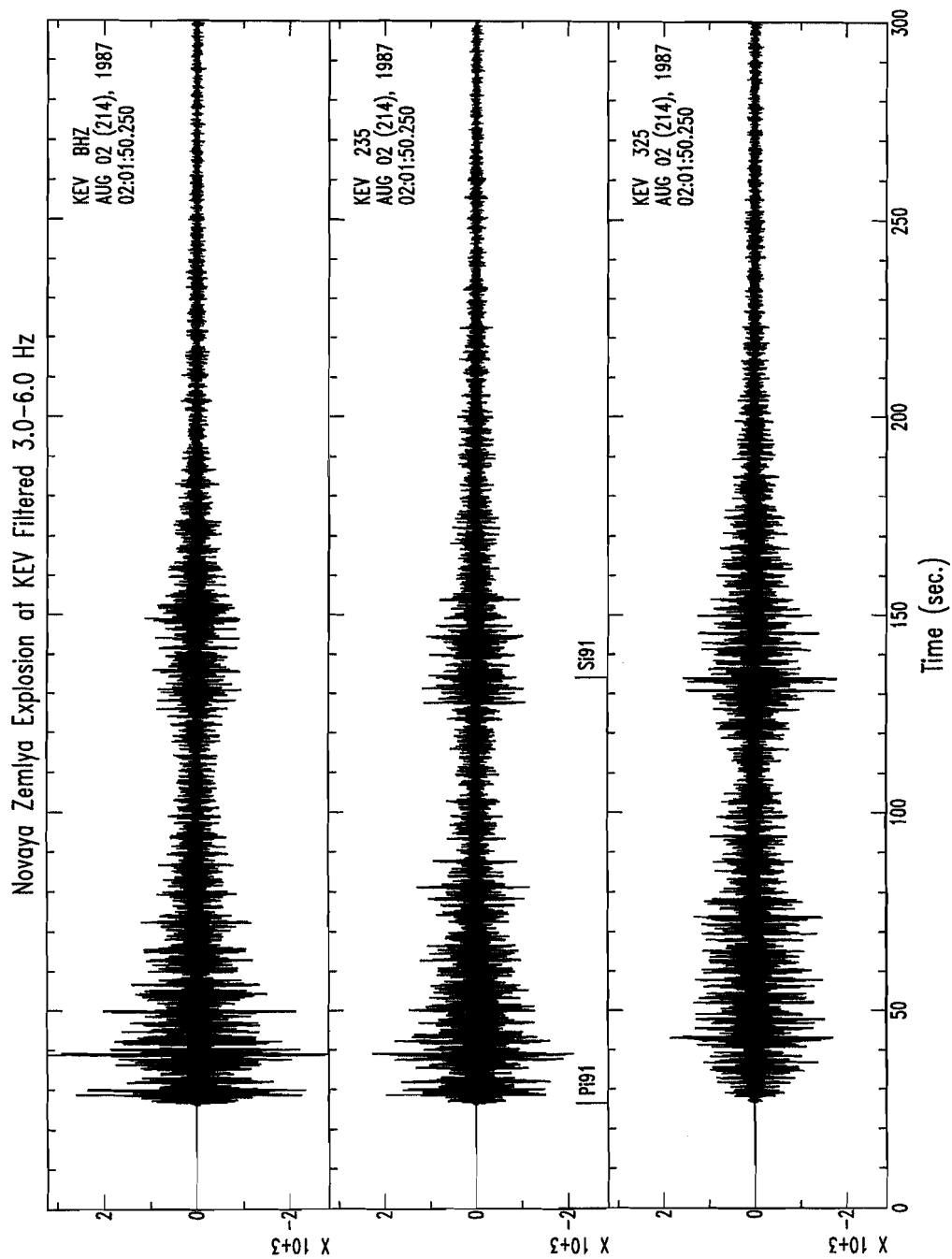


Figure 7a: Three-component seismograms from the 2 August 1987 NNZ explosion recorded at KEV. The components are rotated as described in Figure 6a. PI91 and Si91 are calculated using the origin time and location given in Table 1 and the IASPEI 91 tables. The data are filtered with a passband of 3.0-6.0 Hz.

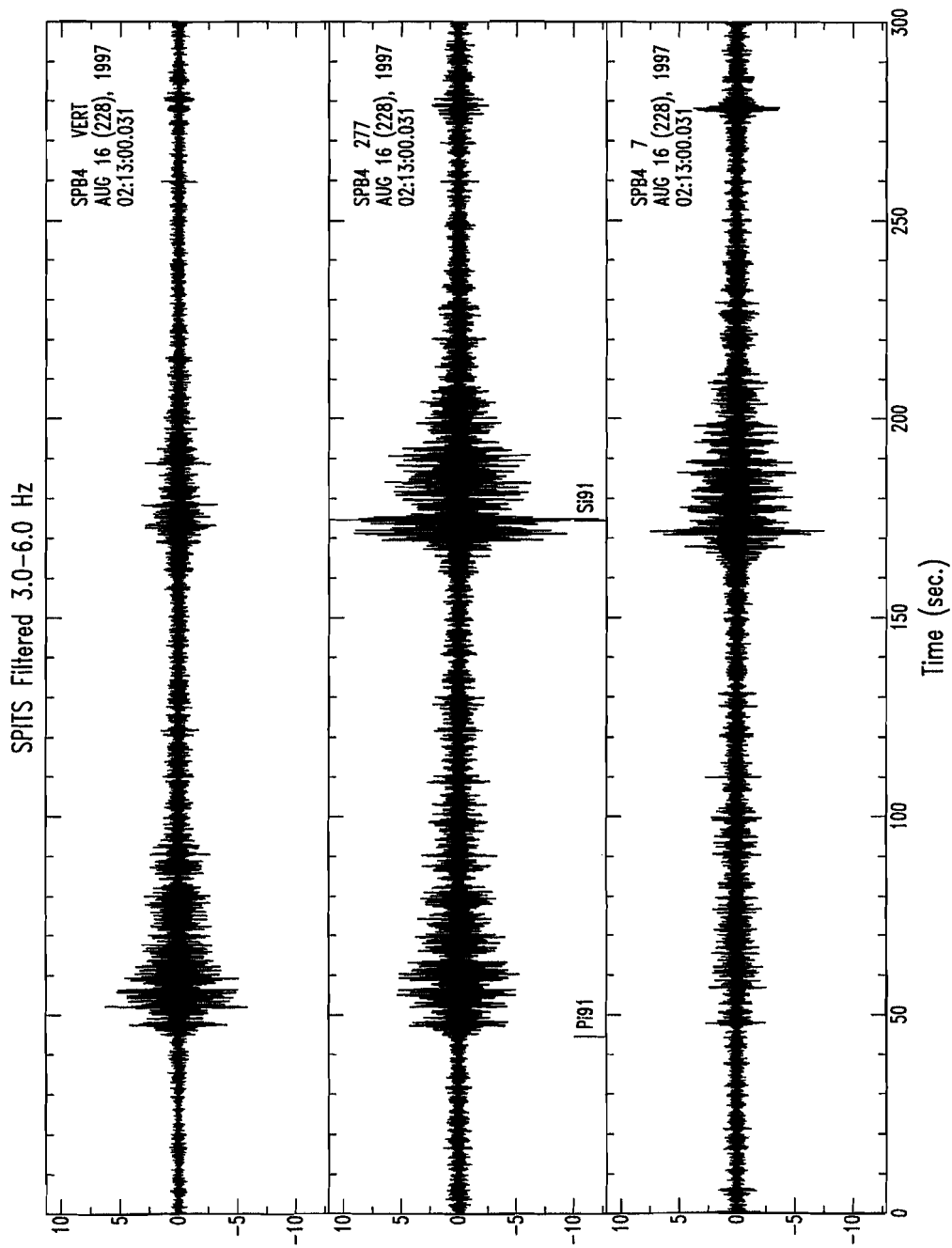


Figure 6d: Three-component seismograms recorded at SPB4 from the 16 August 1997 disturbance. The components are rotated as described in Figure 6a. Pi91 and Si91 are also as described in Figure 6a. The data have been filtered with a passband of 3.0-6.0 Hz.

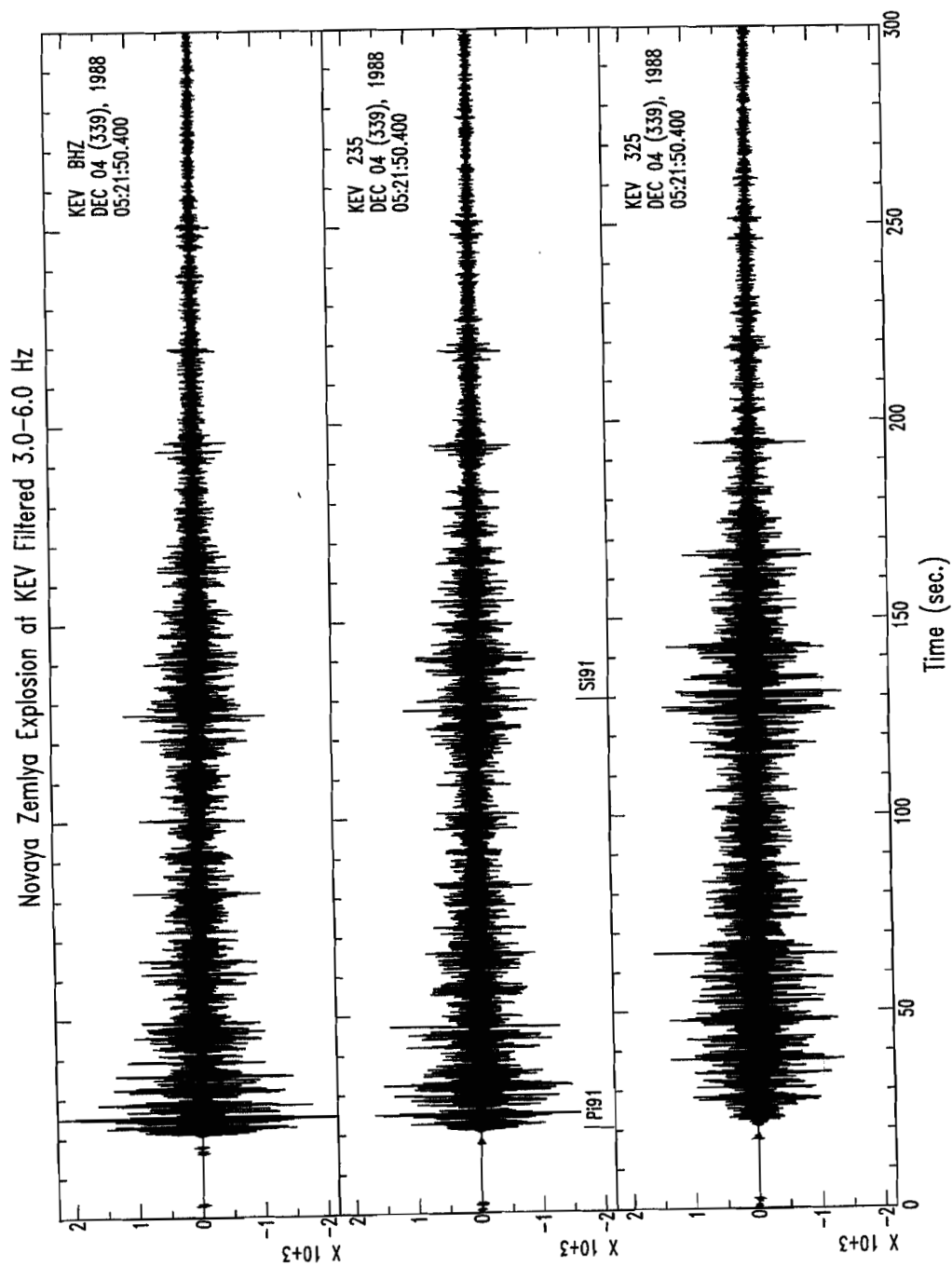


Figure 7c: As Figure 7a, except for the 4 December 1988 NNZ explosion.

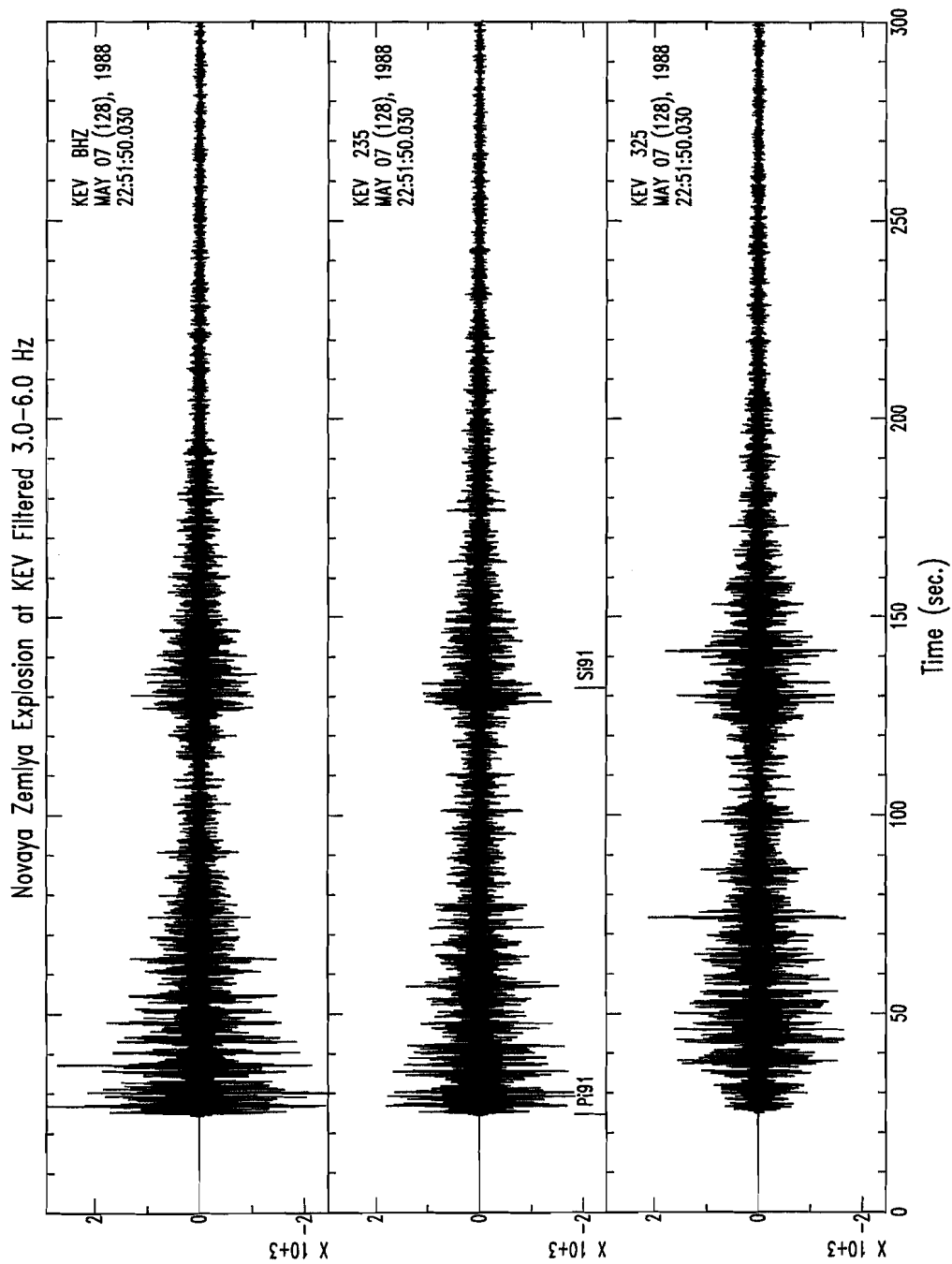


Figure 7b: As Figure 7a, except for the 7 May 1988 NNZ explosion.

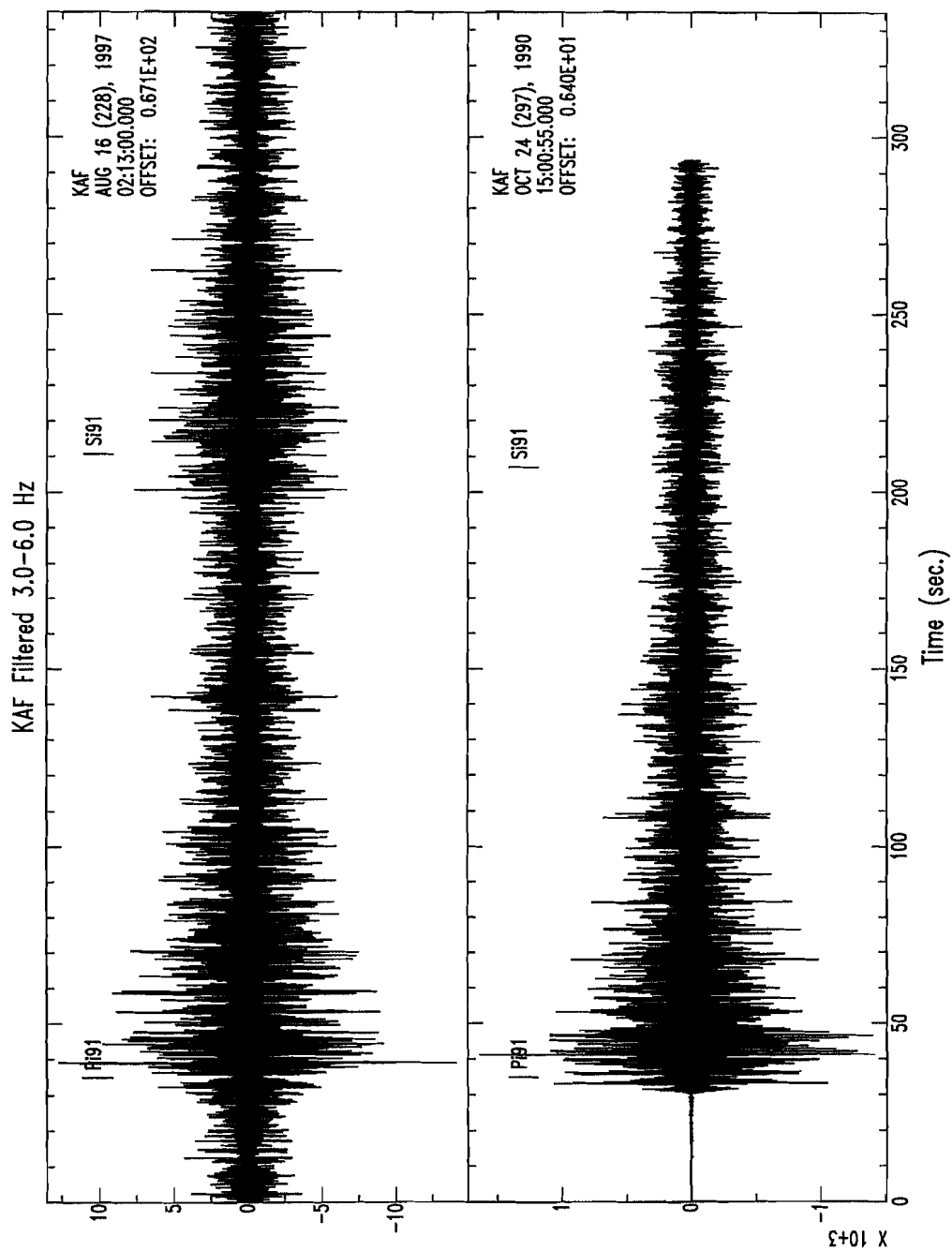


Figure 8: Vertical-component seismograms recorded at KAF from the 16 August 1997 disturbance (upper trace), and the NNZ explosion of 24 October 1990 (lower trace). The data are filtered with a passband of 3.0-6.0 Hz.



Novaya Zemlya Explosion at KEV Filtered 3.0-6.0 Hz

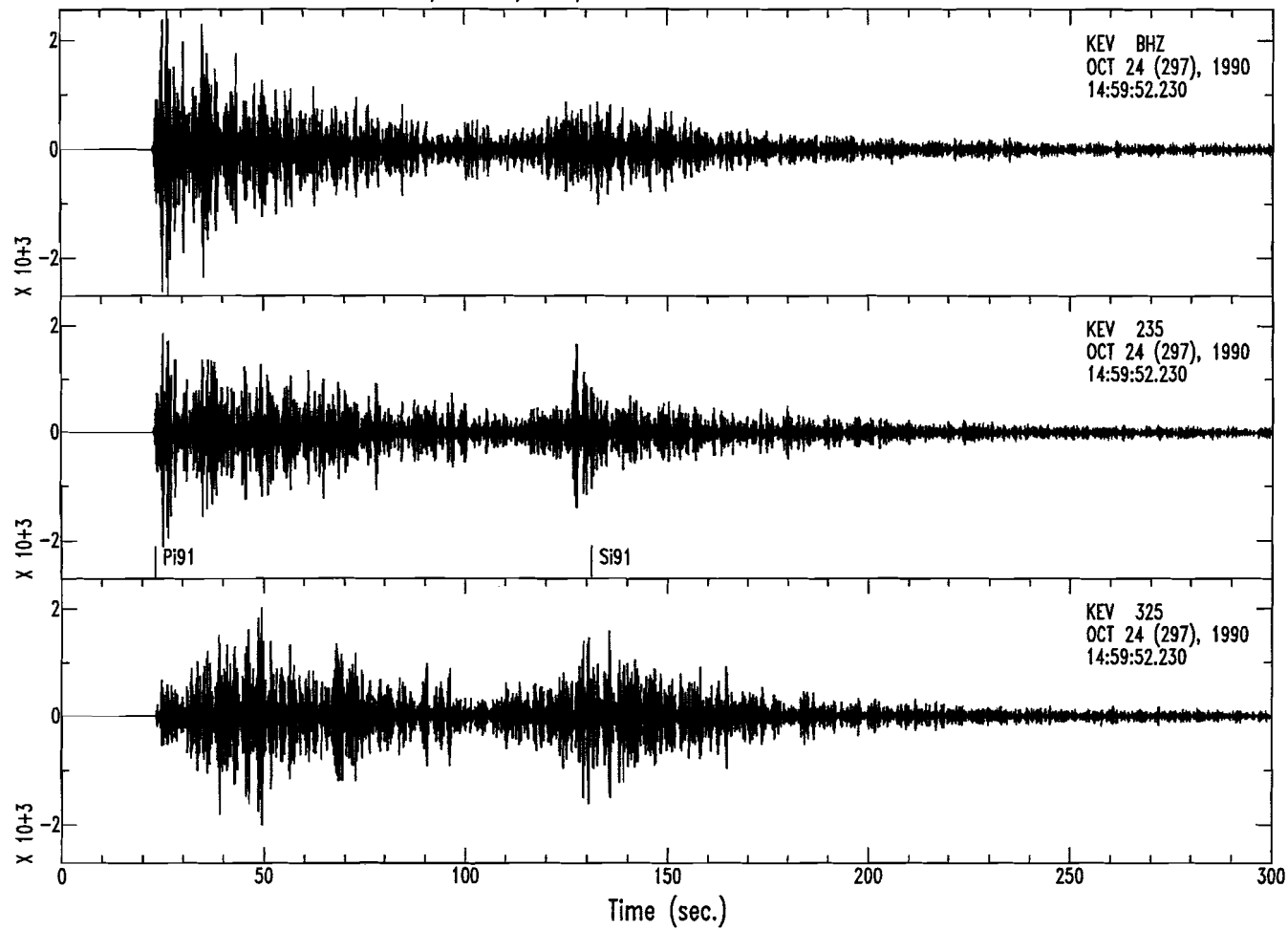


Figure 7d: As Figure 7a, except for the 24 October 1990 NNZ explosion.

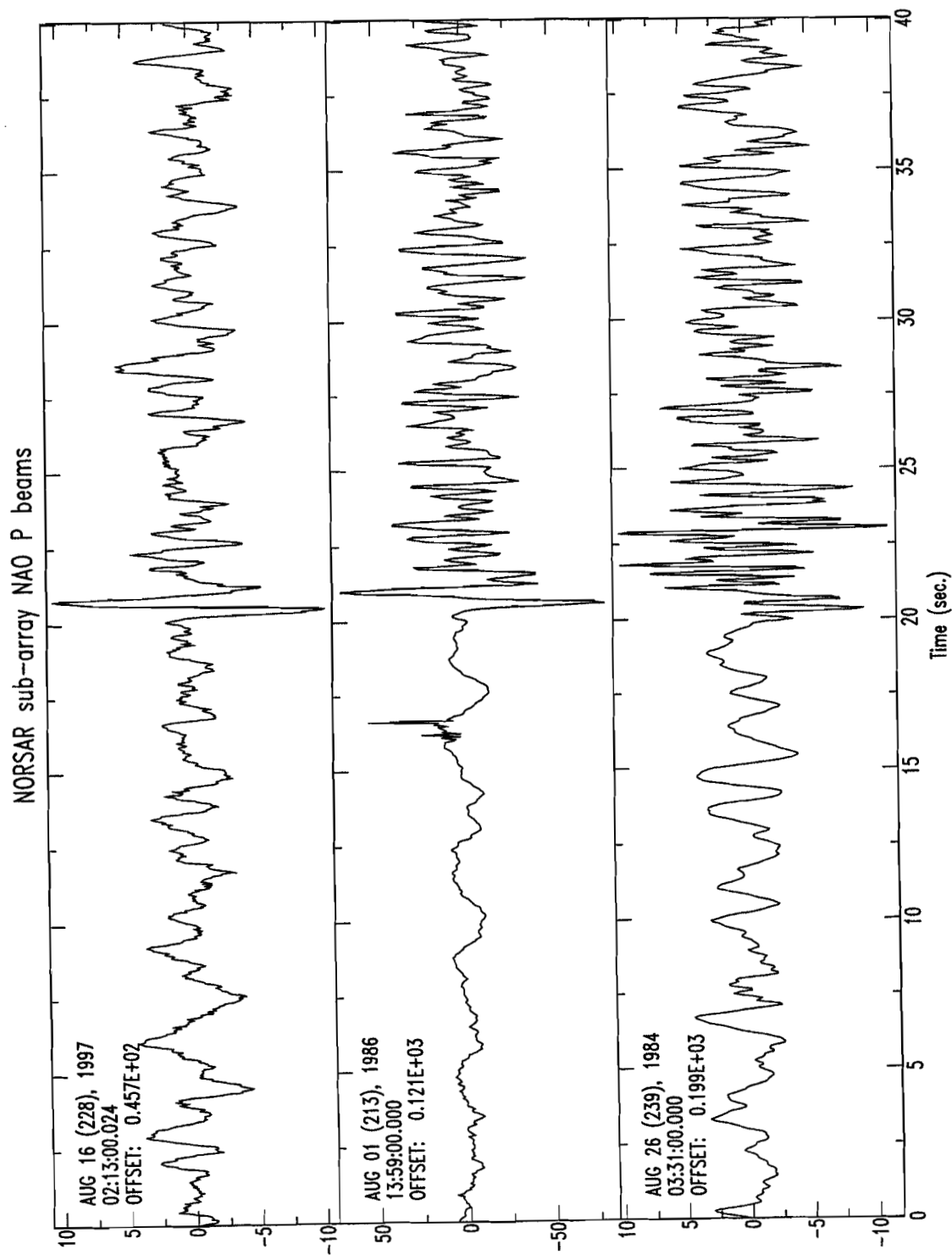


Figure 10a: Comparison of P beams at the NAO subarray of NORSAR. The upper trace is from the 16 August 1997 disturbance, the middle trace is from the 1 August 1986 Kara Sea earthquake, and the lower trace is from a presumed NNZ explosion on 26 August 1984.

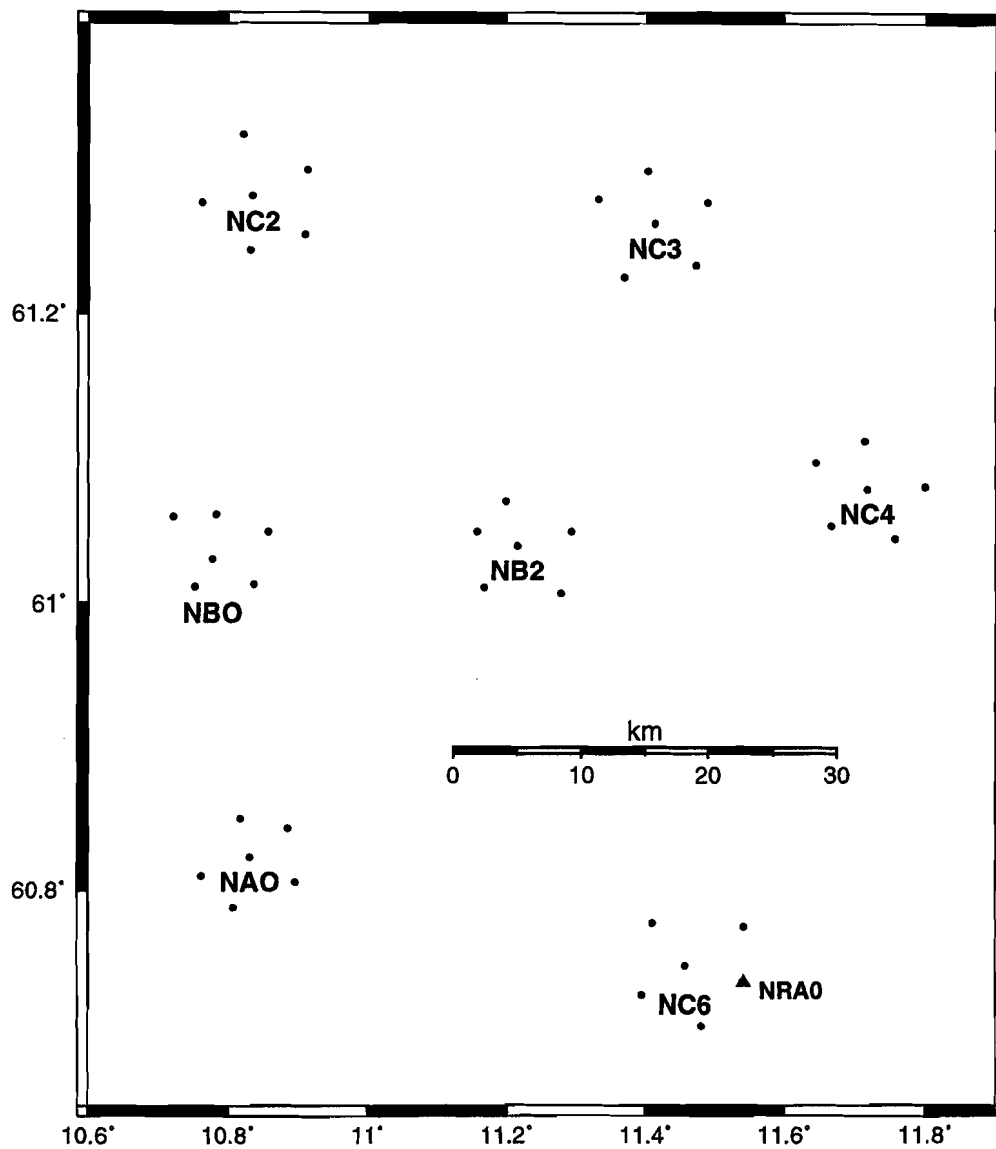


Figure 9: Map showing the location of the subarrays in the large aperture array NOR-SAR. The triangle marks the location of the small aperture array NORES (NRA0).

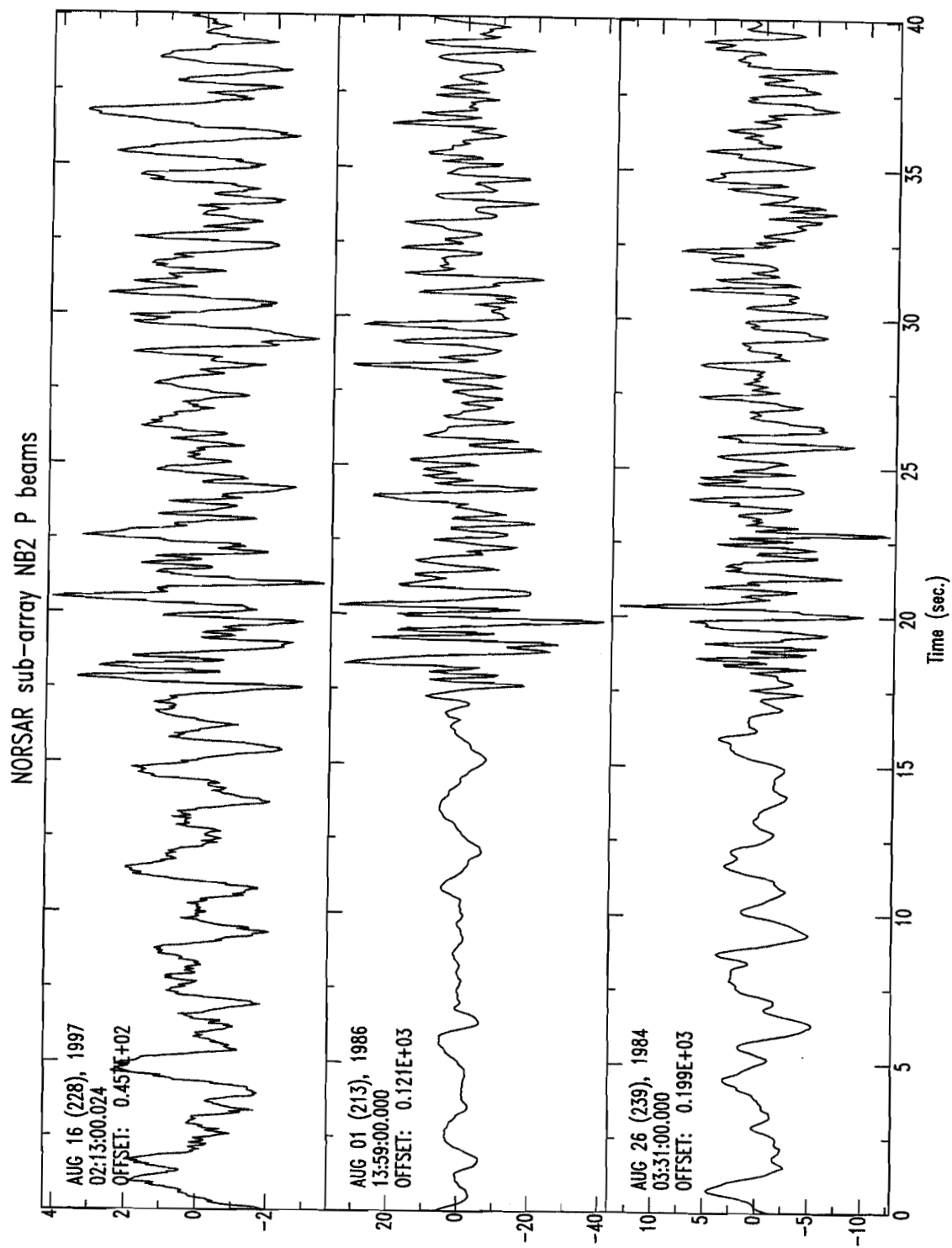


Figure 10c: As Figure 10a, except for NORSAR subarray NB2.

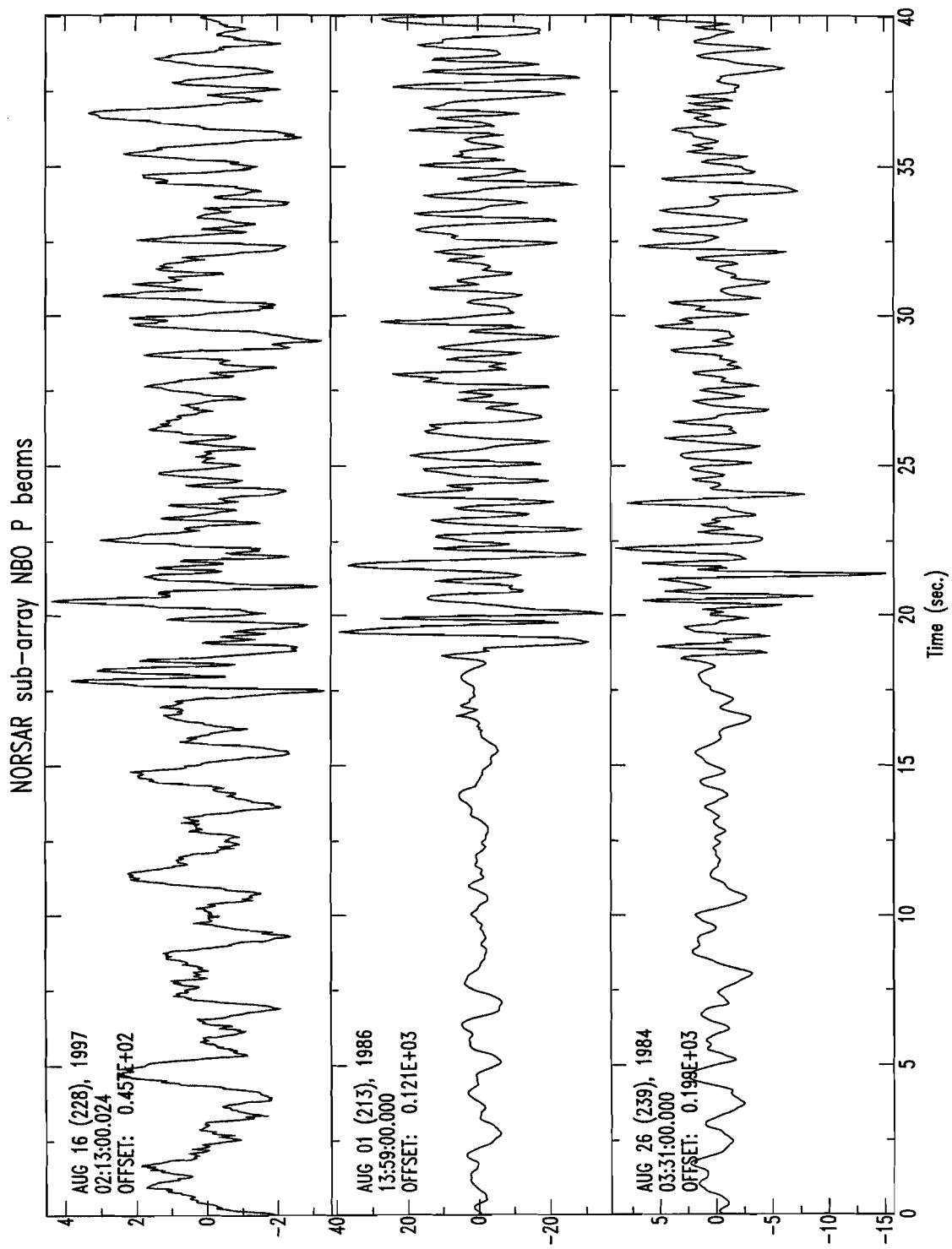


Figure 10b: As Figure 10a, except for NORSAR subarray NBO.

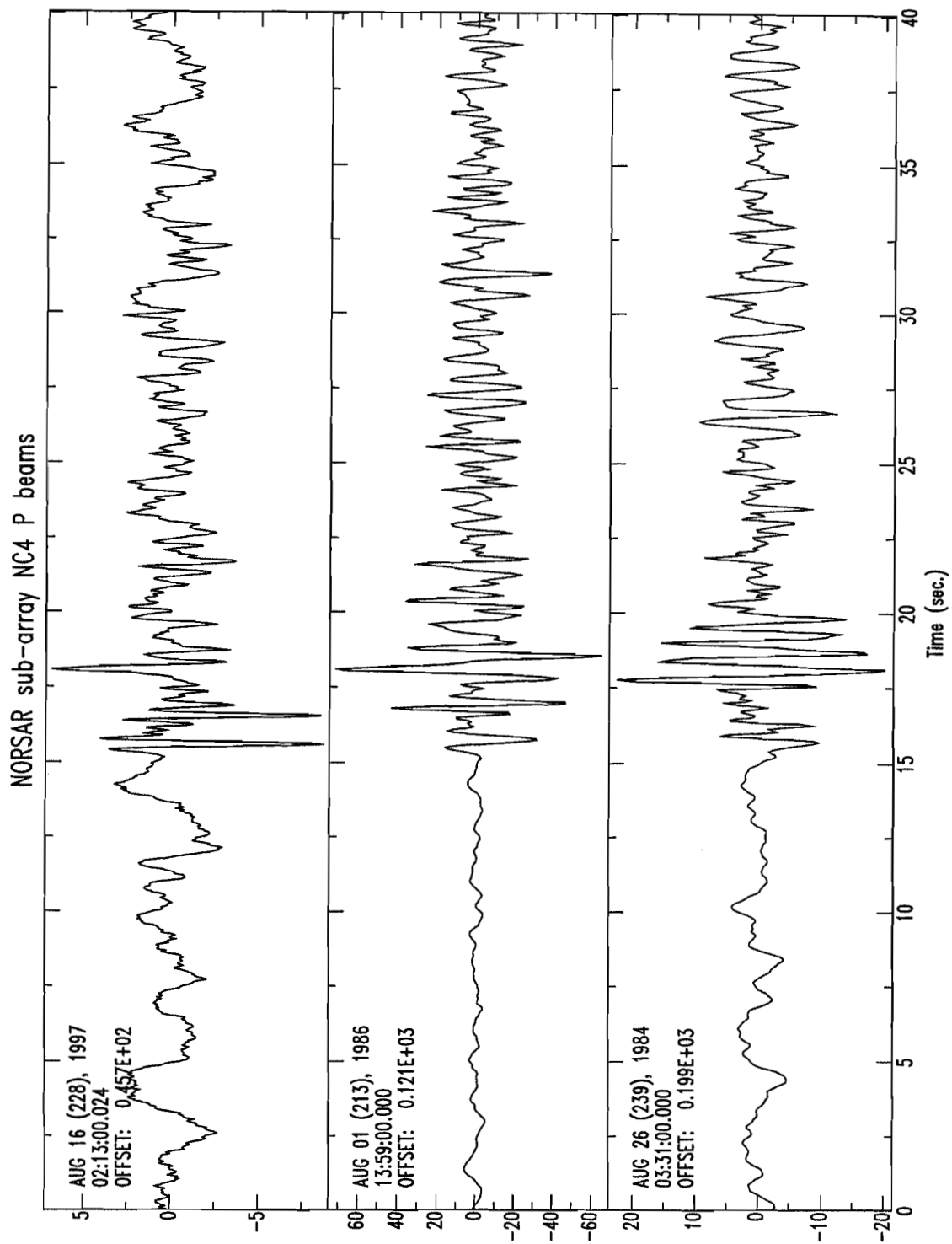


Figure 10e: As Figure 10a, except for NORSAR subarray NC4.

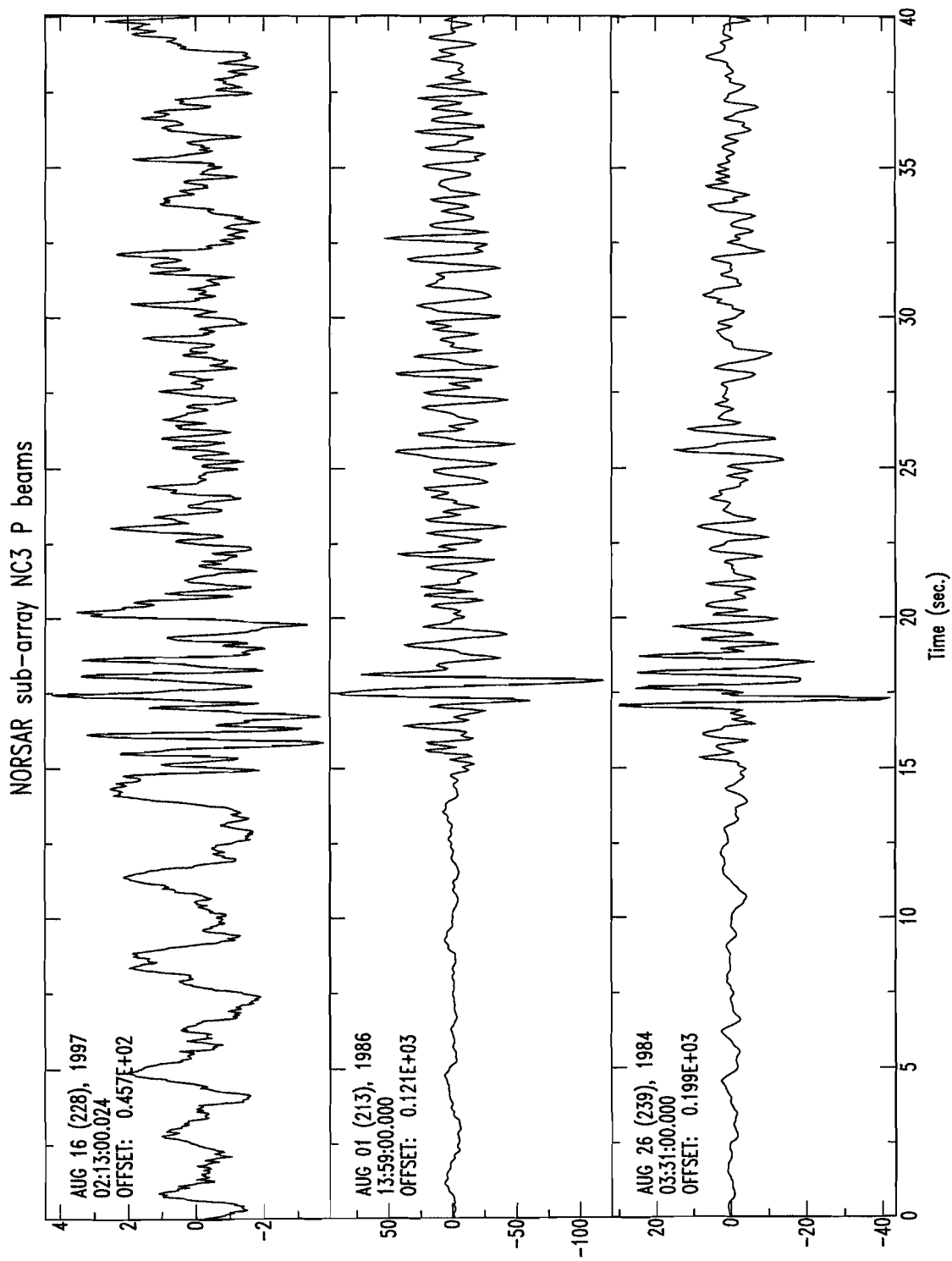


Figure 10d: As Figure 10a, except for NORSAR subarray NC3.

## Appendix A

- Figure A1 Vertical component waveforms from each subarray in NORSAR from the 16 August 1997 disturbance, along with the subarray beam. (a) NAO, (b) NBO, (c) NB2, (d) NC2, (e) NC3, (f) NC4, and (g) NC6.
- Figure A2 As Figure A1 except for the 1 August 1986 Kara Sea earthquake. (a) NAO, (b) NBO, (c) NB2, (d) NC3, (e) NC4, and (f) NC6.
- Figure A3 As Figure A1 except for the presumed NNZ explosion of 26 August 1984. (a) NAO, (b) NBO, (c) NB2, (d) NC2, (e) NC3, and (f) NC4.



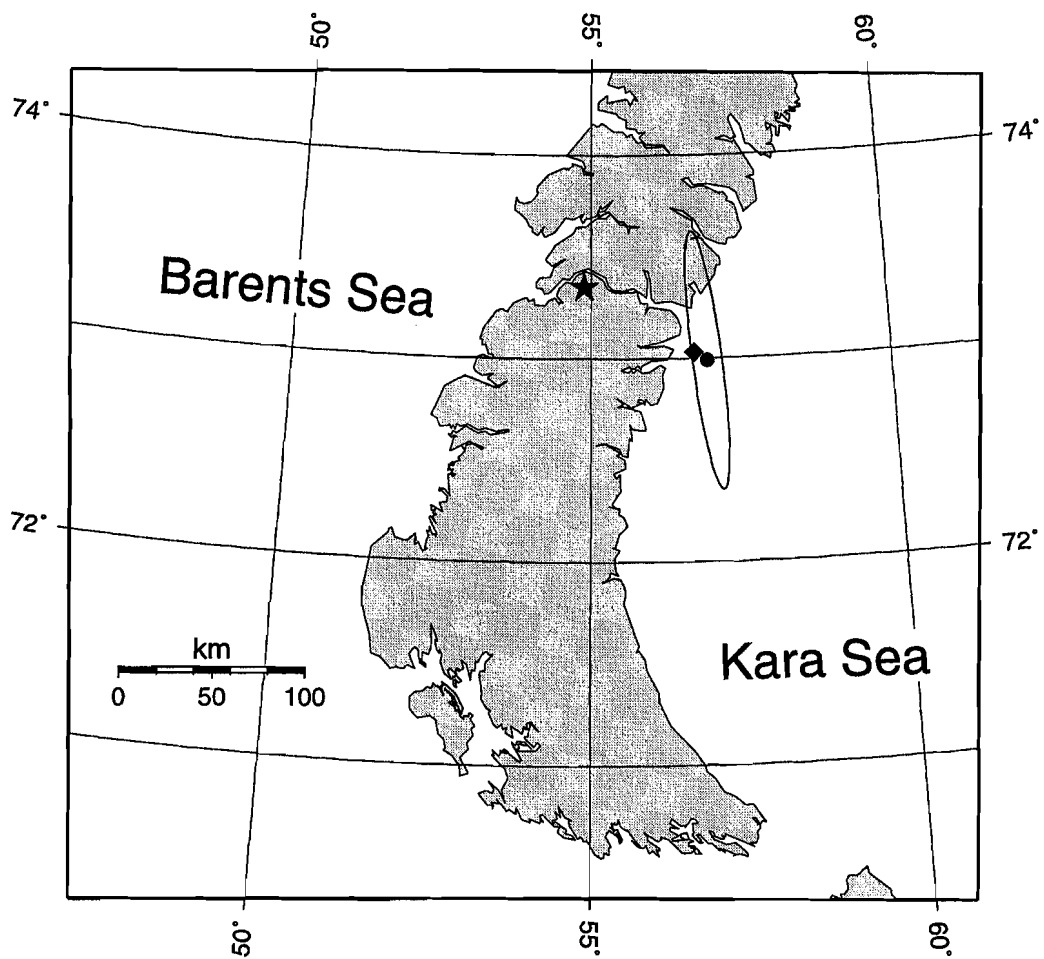


Figure 11: Map showing the location of NNZ, the epicentre of the 1 August 1986 Kara Sea earthquake determined by Marshall et al. (1989) (diamond), and the JED epicentre of the 16 August 1997 disturbance determined by R.G. North (written communication) (circle). The 90% confidence ellipse for the 16 August 1997 JED epicentre is also shown.

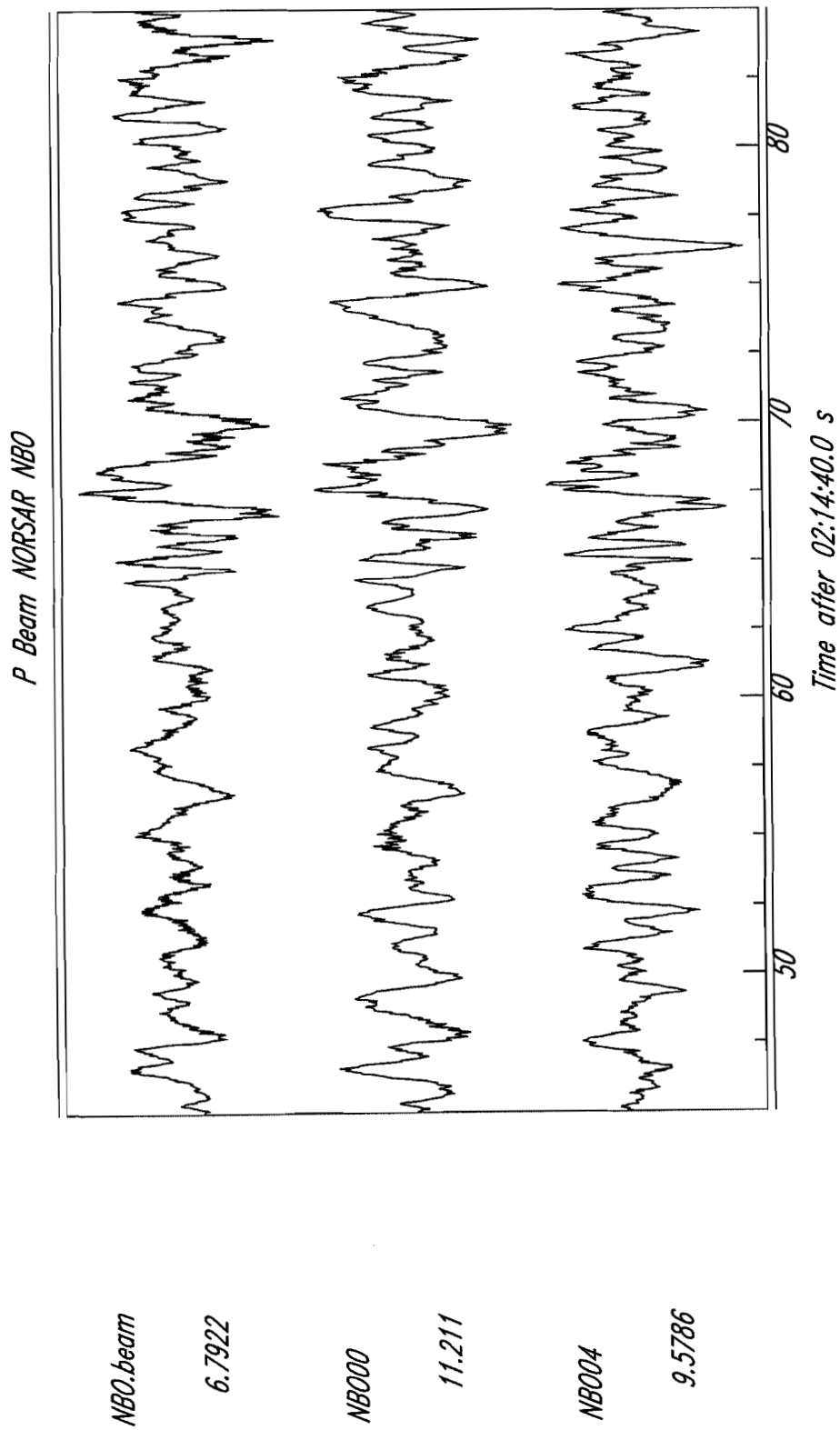


Figure A1b: As Figure A1a, except for NORSAR subarray NBO

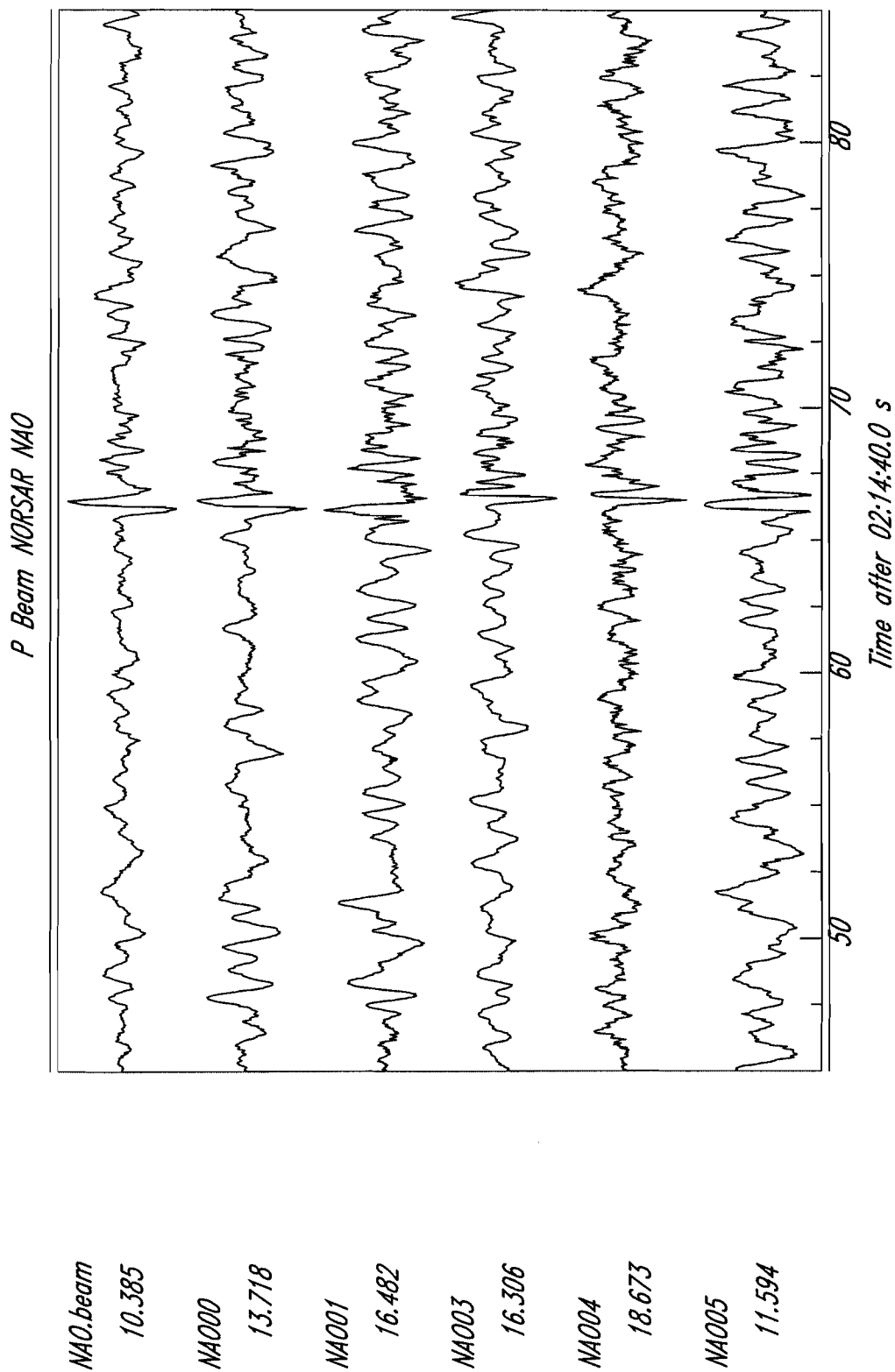


Figure A1a: Vertical-component *P* waveforms recorded at each element in NORSAR subarray NAO from the 16 August 1997 disturbance used to form the subarray beam (upper trace).

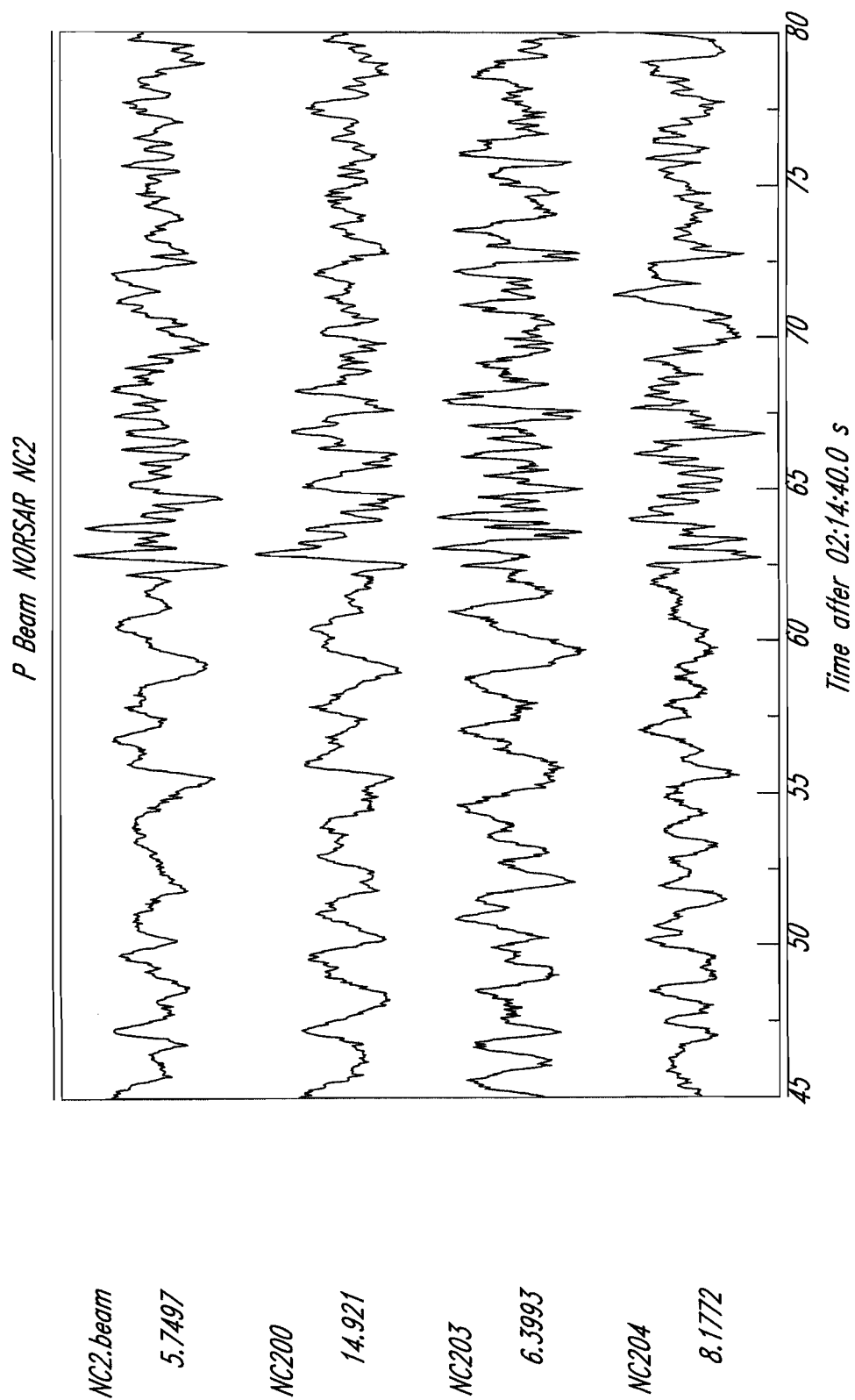


Figure A1d: As Figure A1a, except for NORSAR subarray NC2

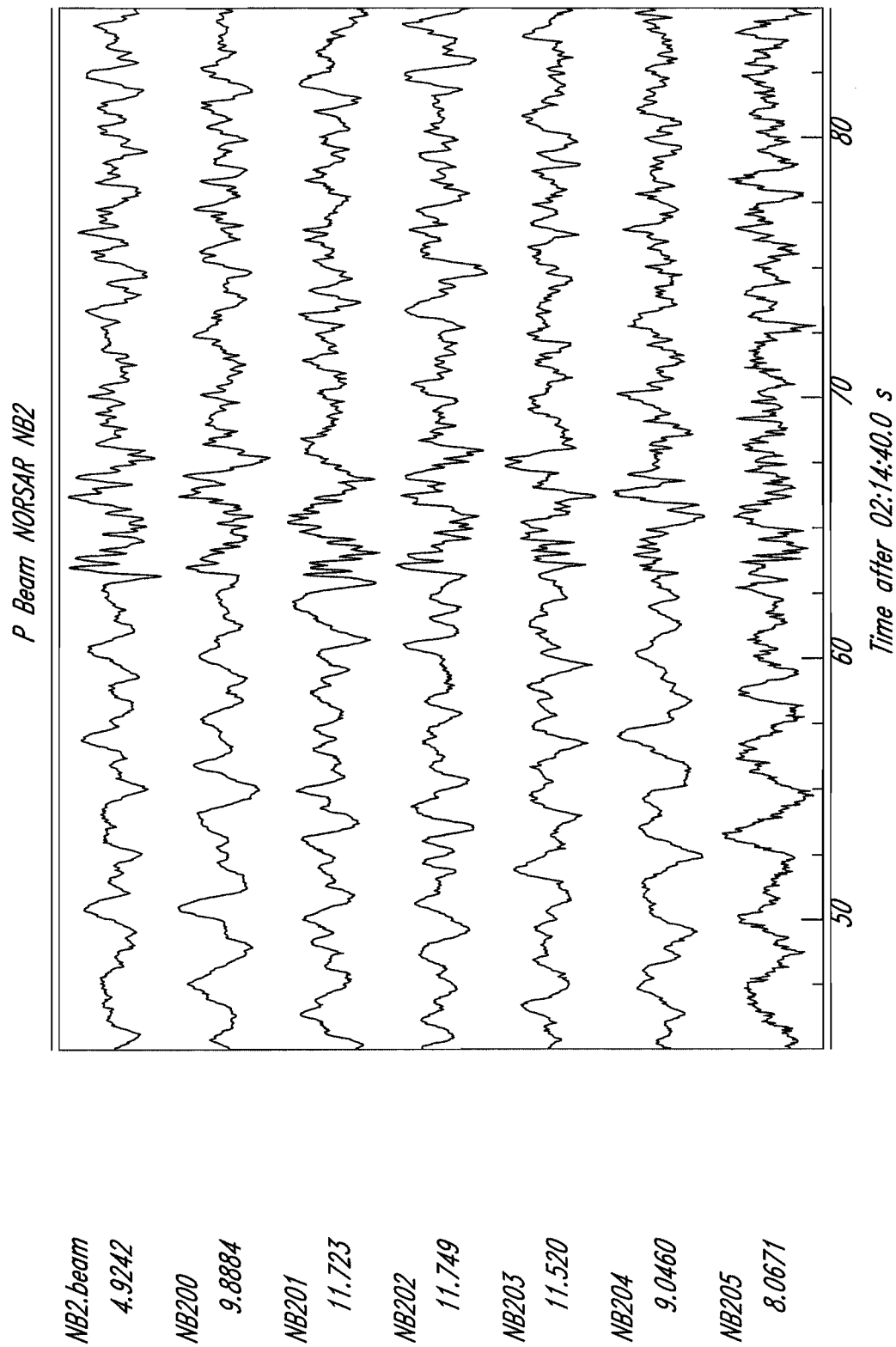


Figure A1c: As Figure A1a, except for NORSAR subarray NB2

*P Beam NORSAR NC4*

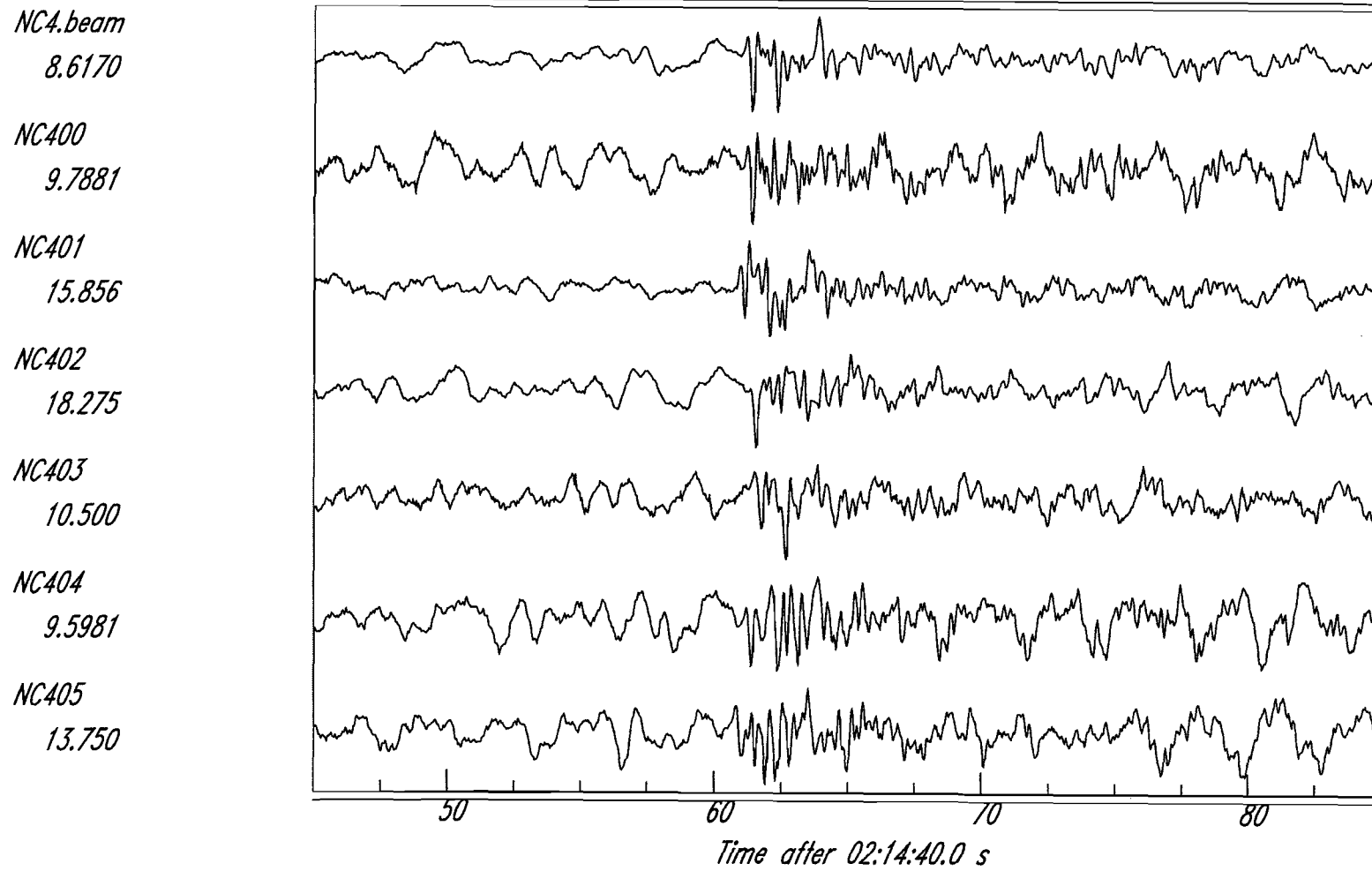


Figure A1f: As Figure A1a, except for NORSAR subarray NC4

*P Beam NORSAR NC3*

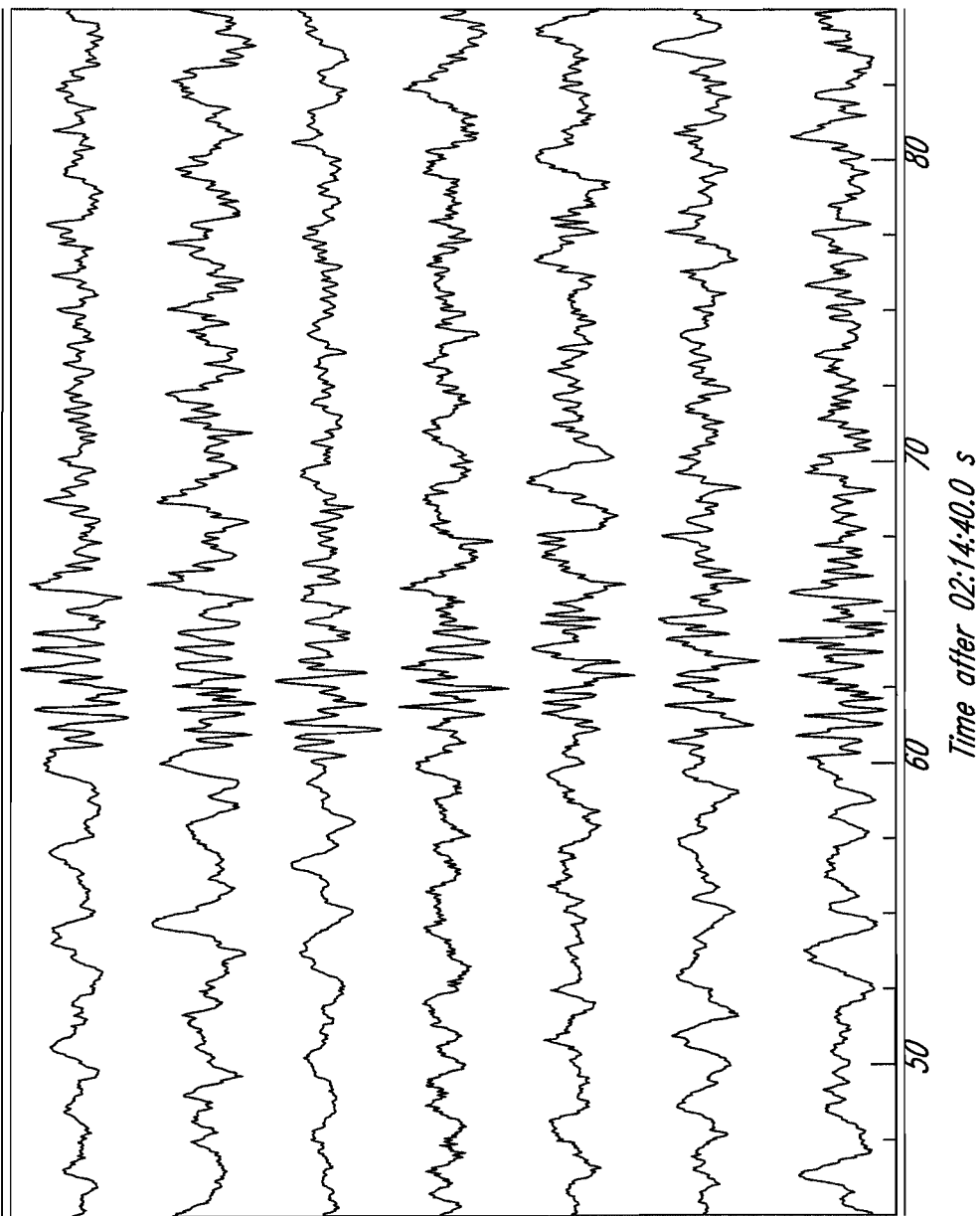


Figure A1e: As Figure A1a, except for NORSAR subarray NC3

*P Beam NORSAR NAO*

*NAO.beam*

*80.361*

*NA000*

*71.394*

*NA002*

*173.53*

*NA003*

*110.68*

*NA005*

*94.282*

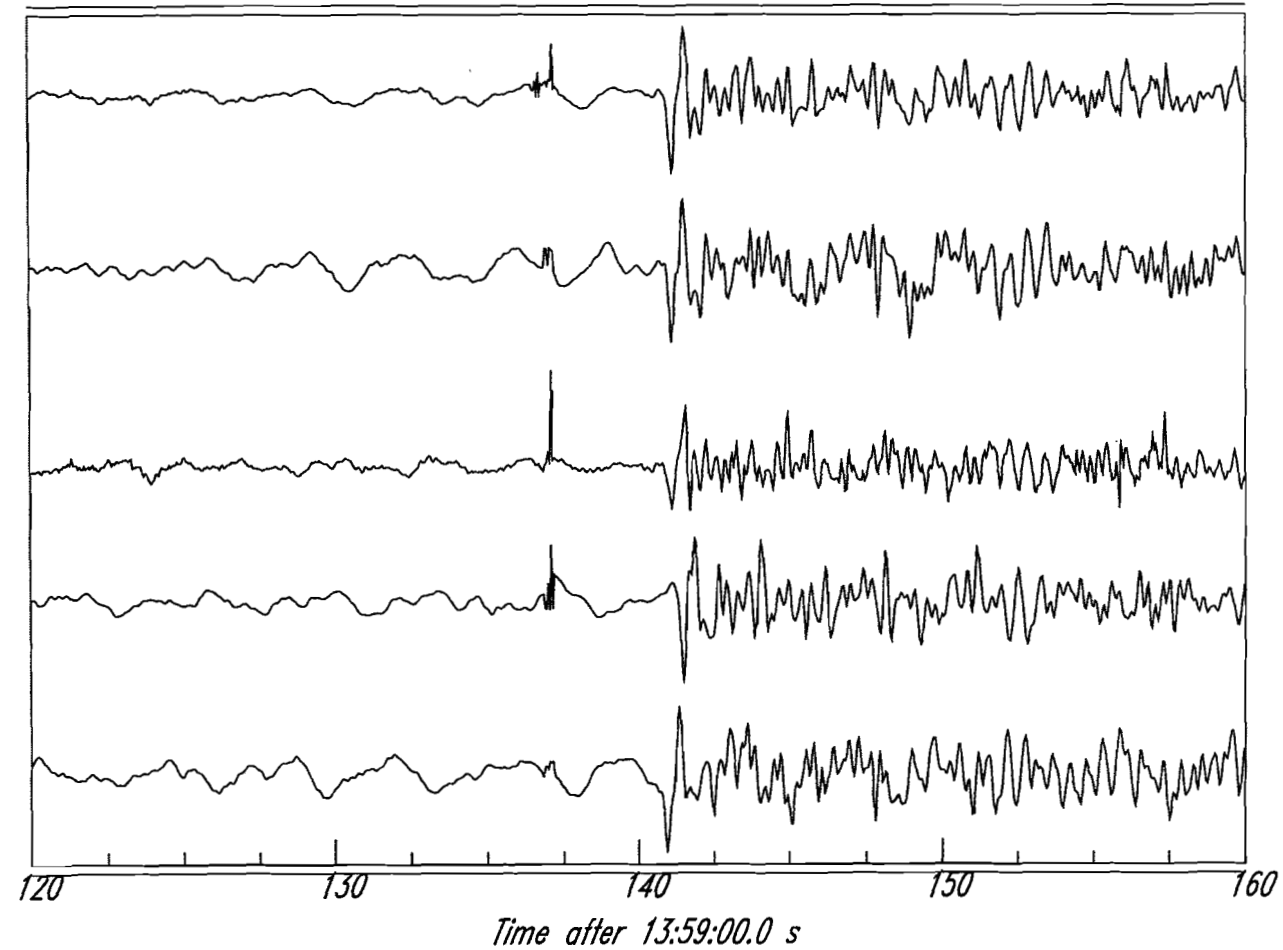


Figure A2a: Vertical-component *P* waveforms recorded at each element in NORSAR subarray NAO from the 1 August 1986 Kara Sea earthquake used to form the subarray beam (upper trace).



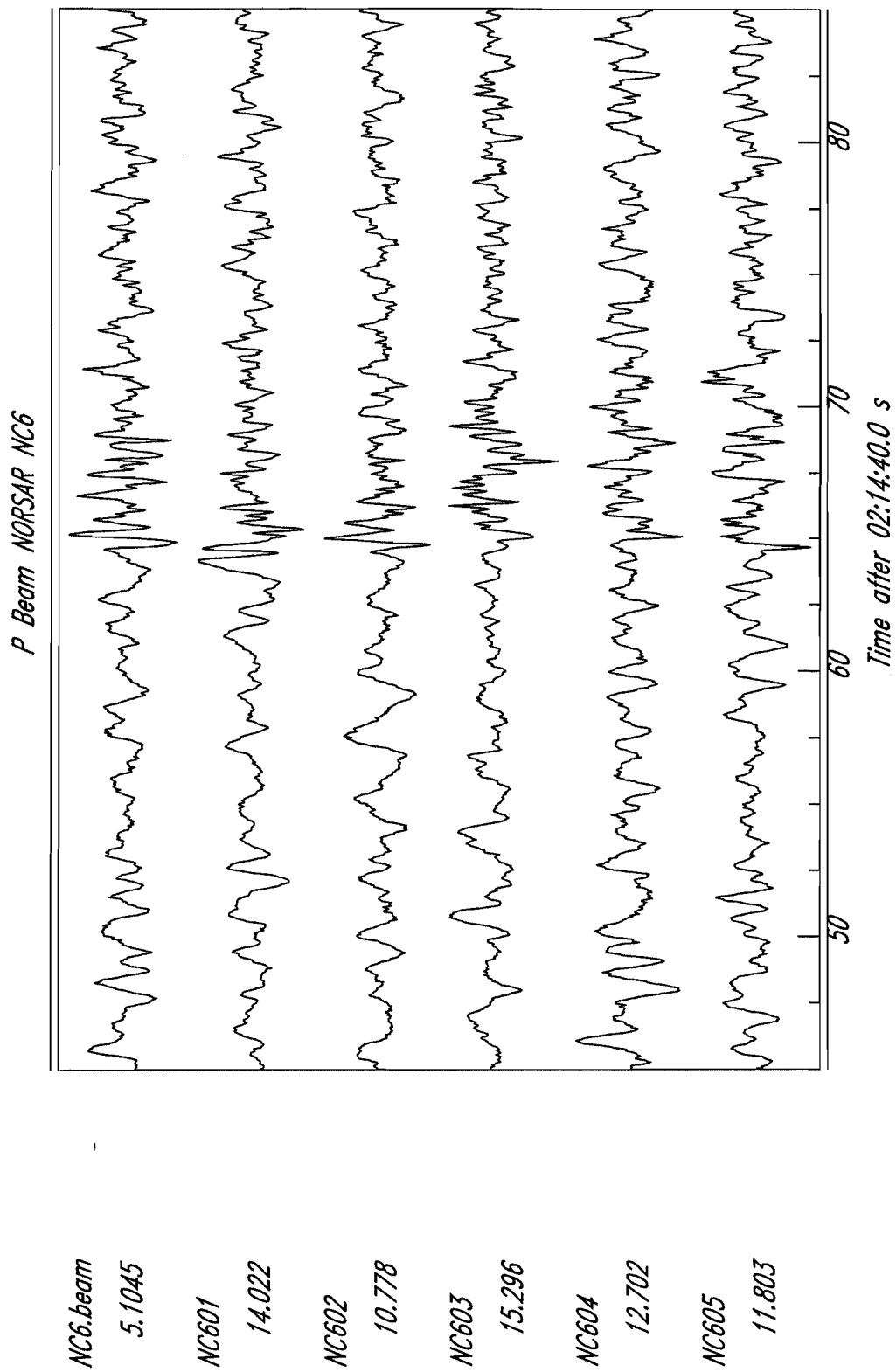


Figure A1g: As Figure A1a, except for NORSAR subarray NC6

*P Beam NORSAR NB2*

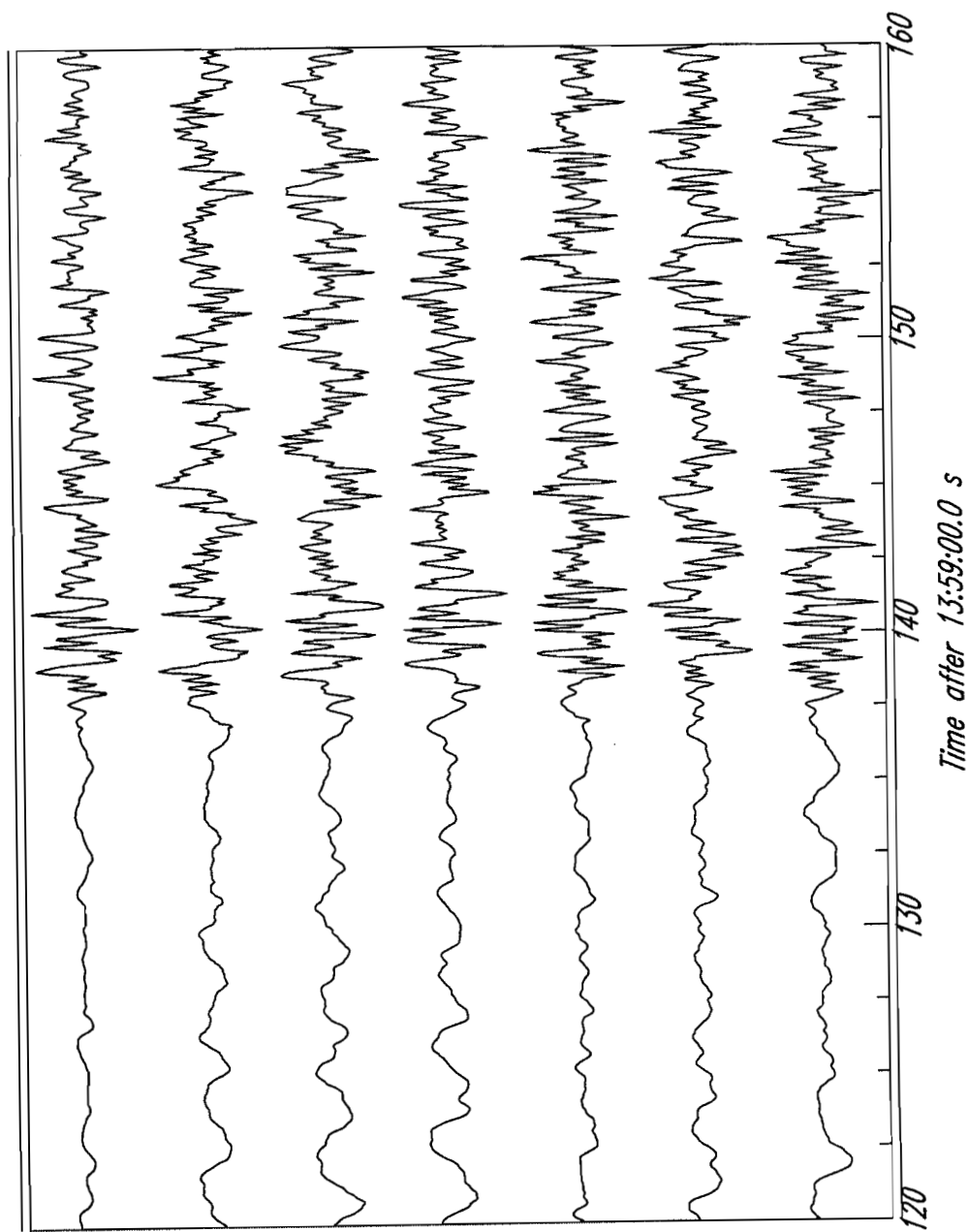


Figure A2c: As Figure A2a, except for NORSAR subarray NB2

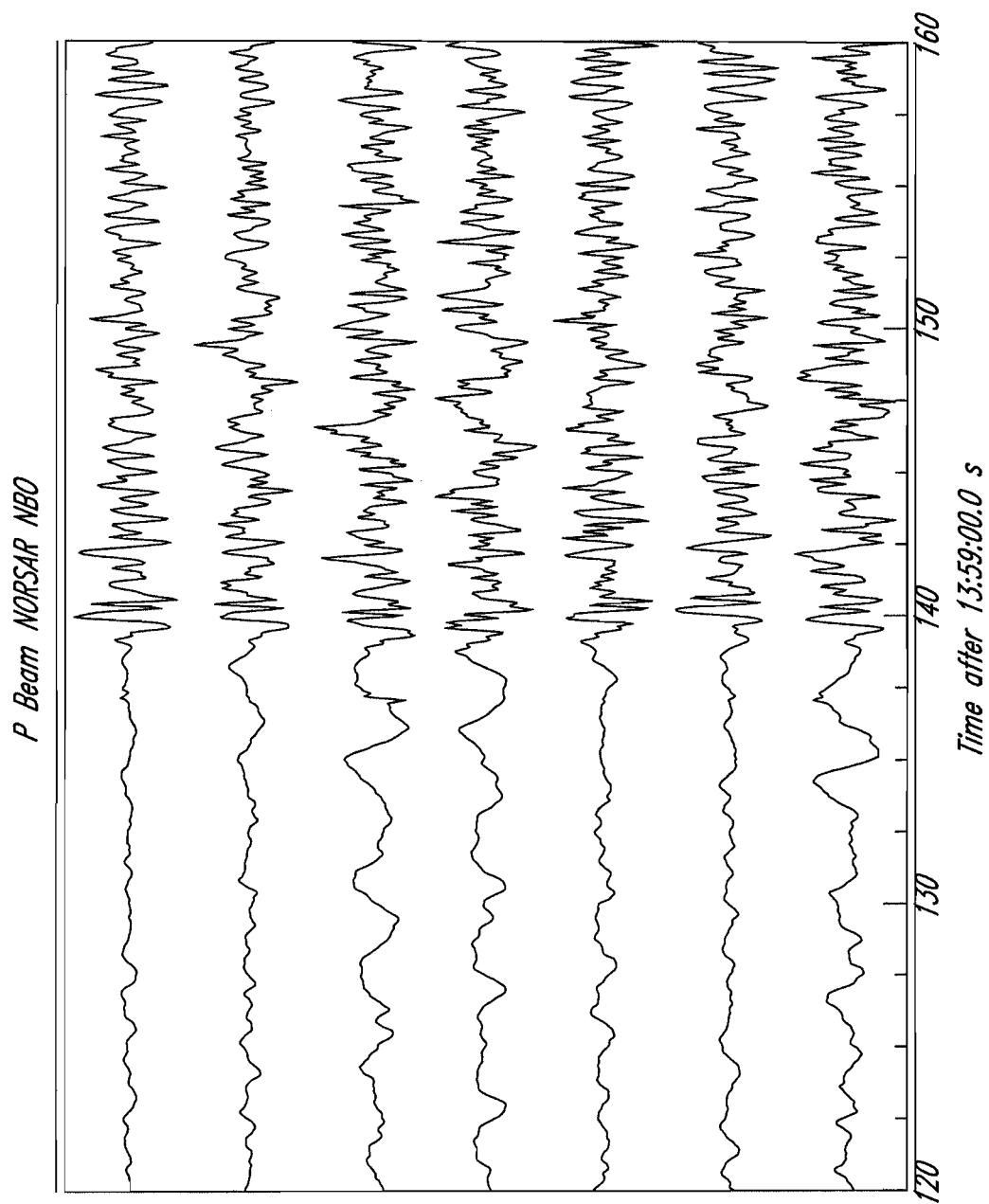


Figure A2b: As Figure A2a, except for NORSAR subarray NBO

*P Beam NORSAR NC4*

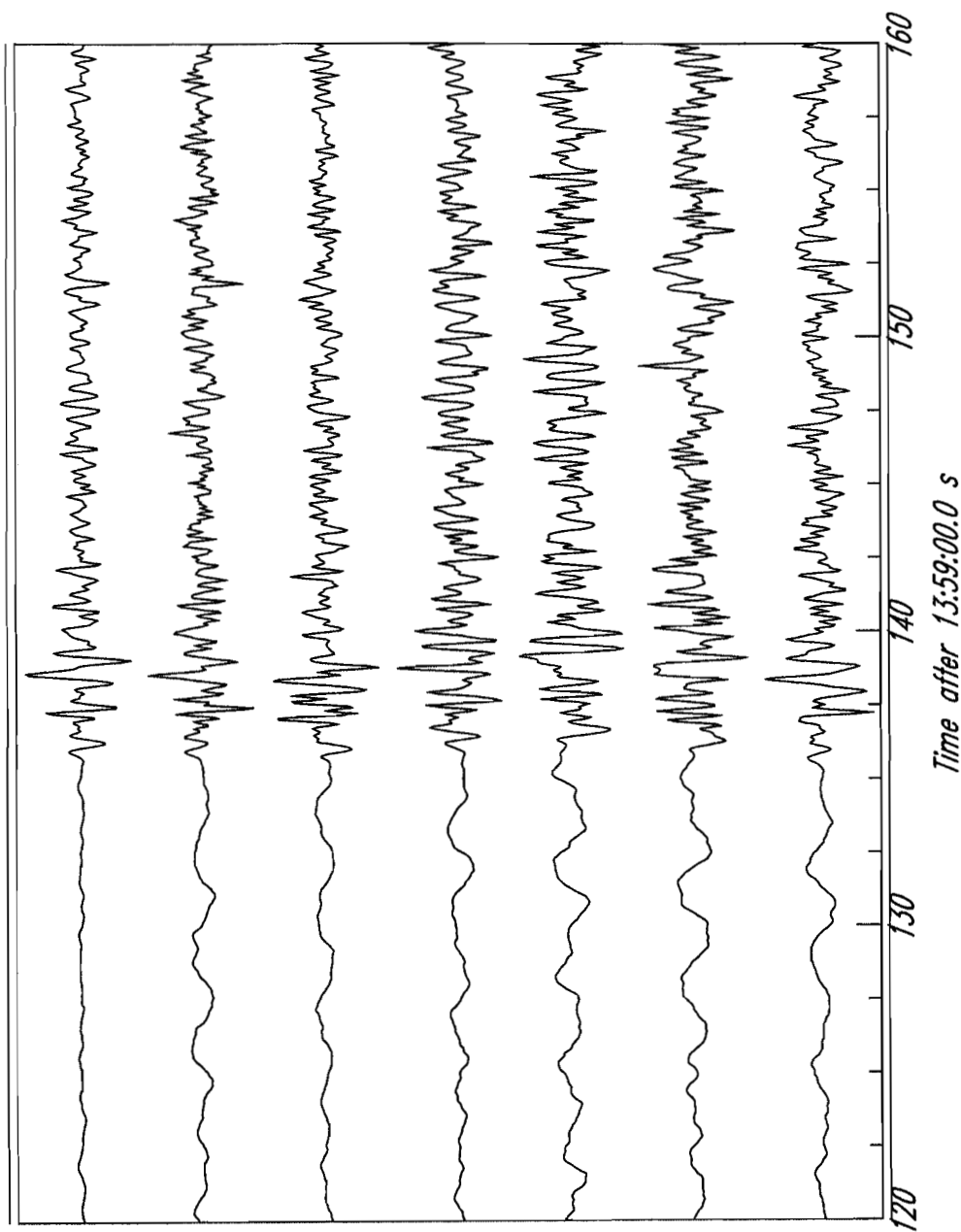


Figure A2e: As Figure A2a, except for NORSAR subarray NC4

*P Beam NORSAR NC6*

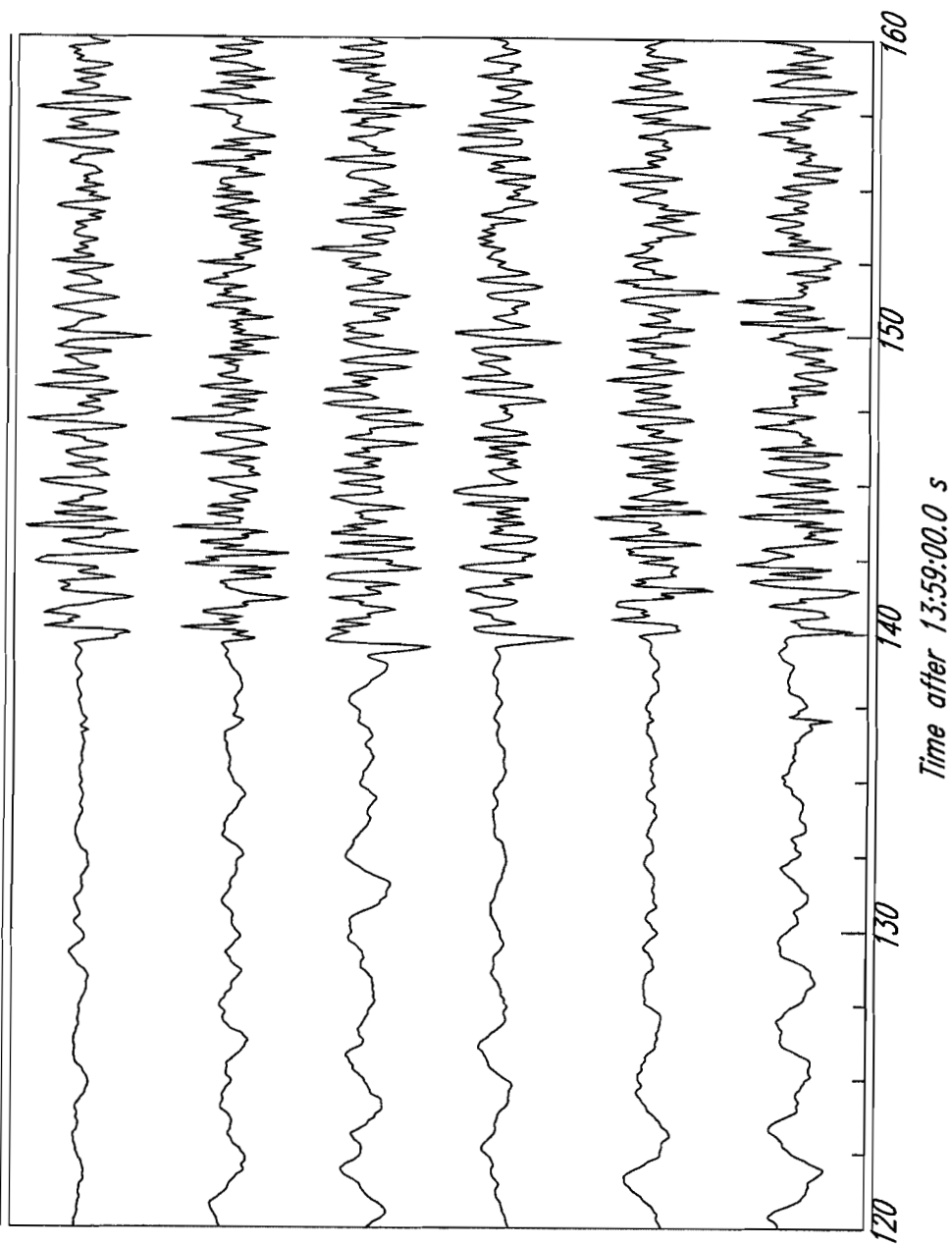


Figure A2f: As Figure A2a, except for NORSAR subarray NC6

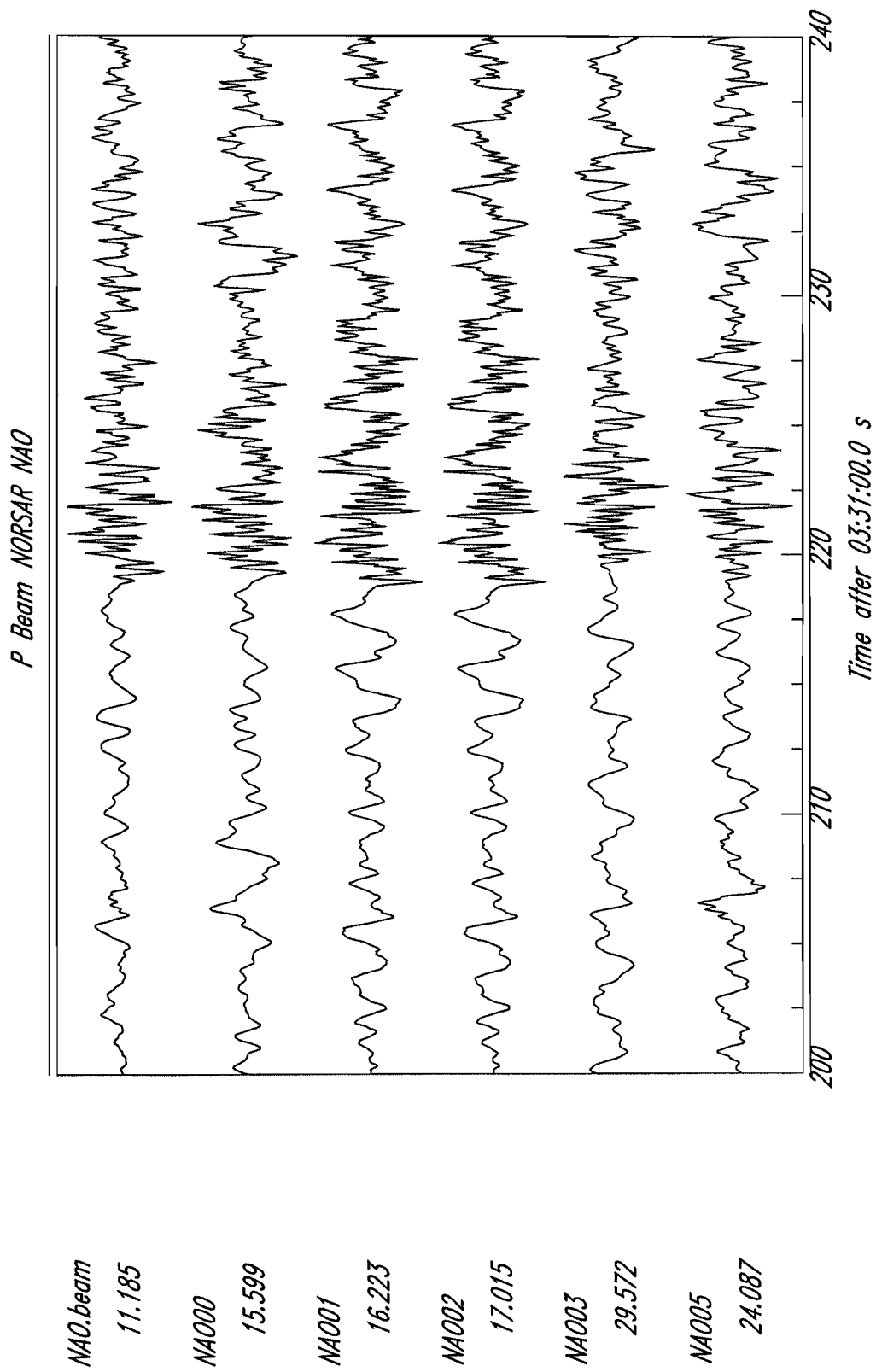


Figure A3a: Vertical-component *P* waveforms recorded at each element in NORSAR subarray NAO from the presumed NNZ explosion on 26 August 1984 used to form the subarray beam (upper trace).

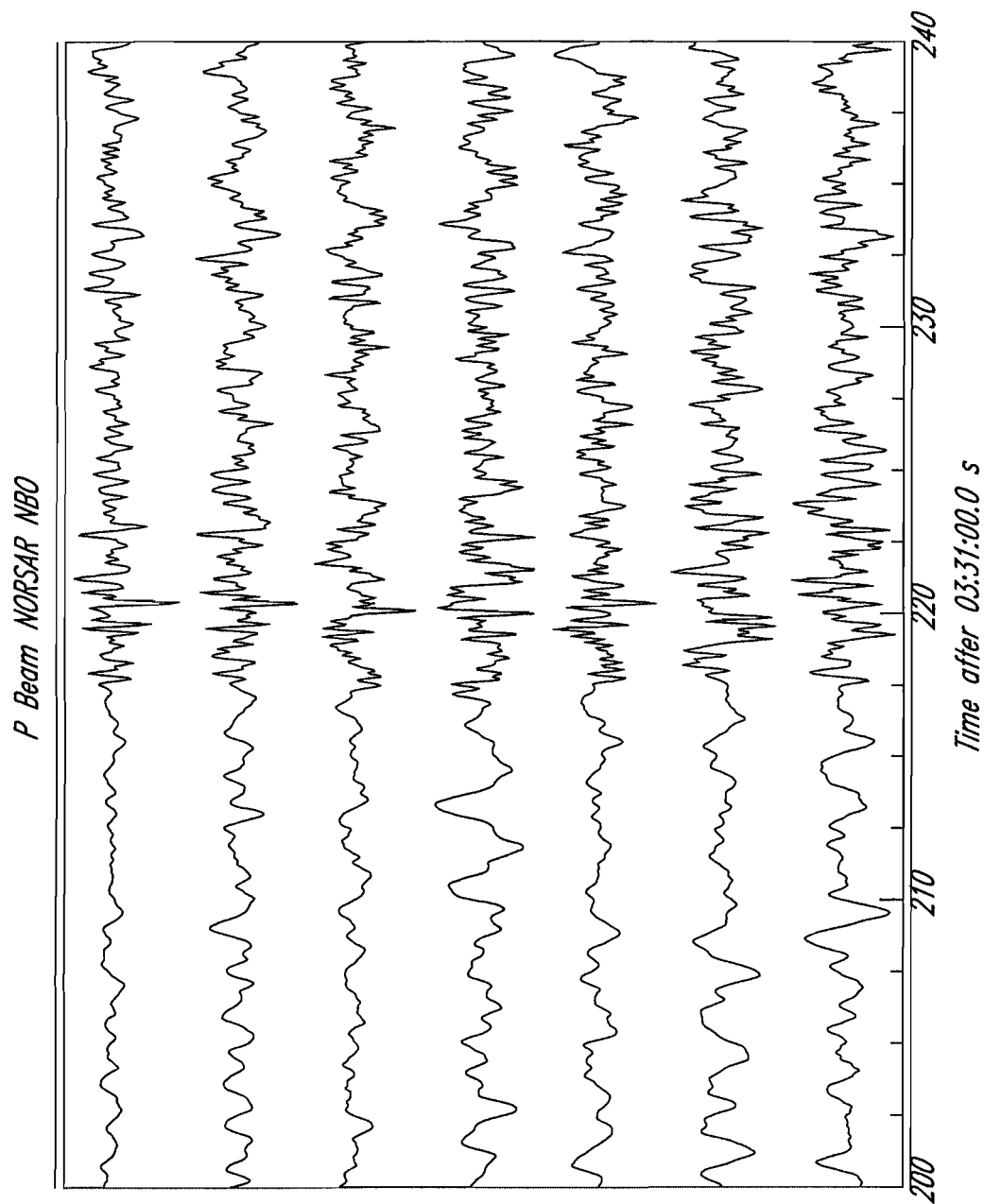


Figure A3b: As Figure A3a, except for NORSAR subarray NBO

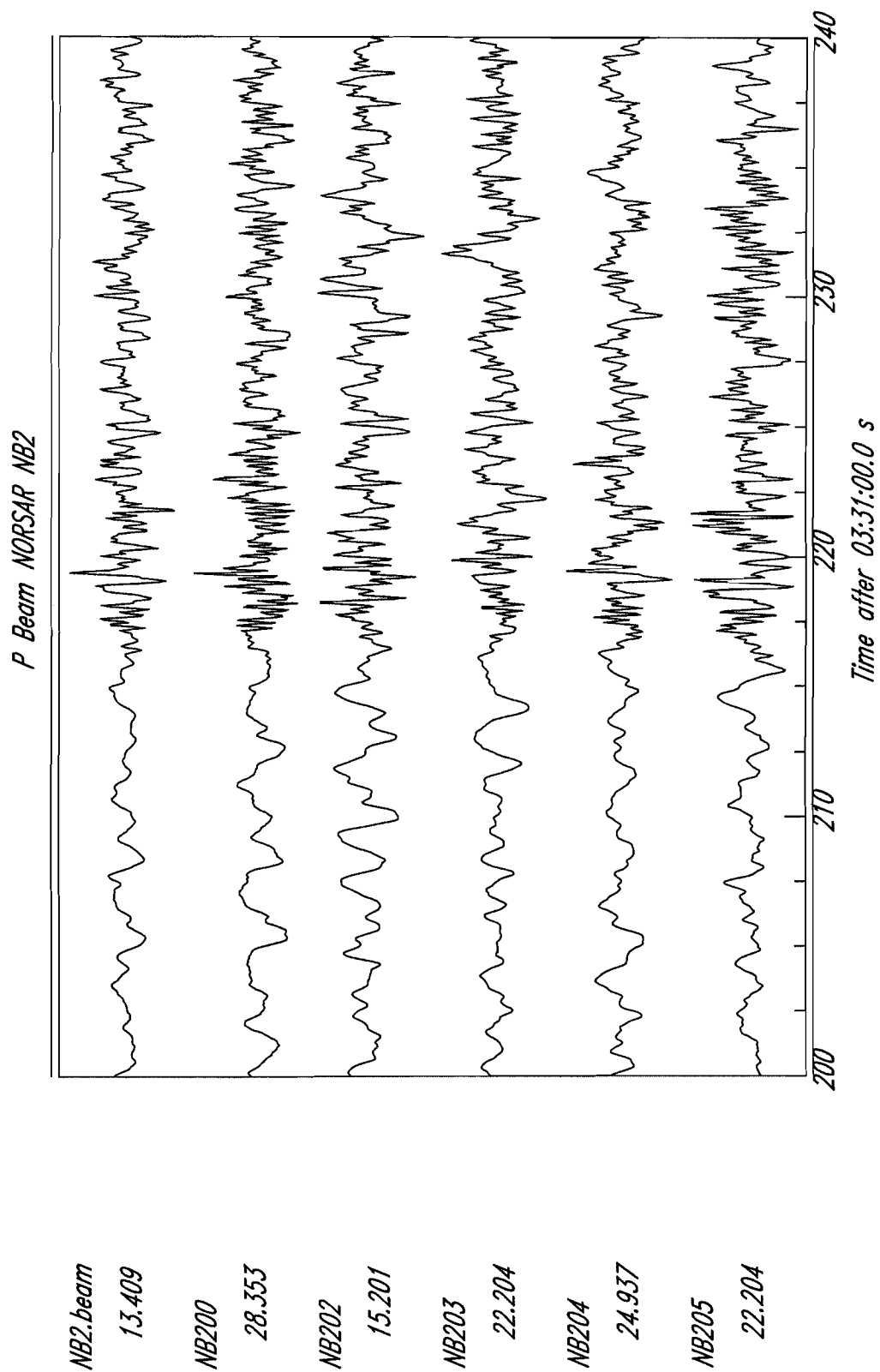


Figure A3c: As Figure A3a, except for NORSAR subarray NB2



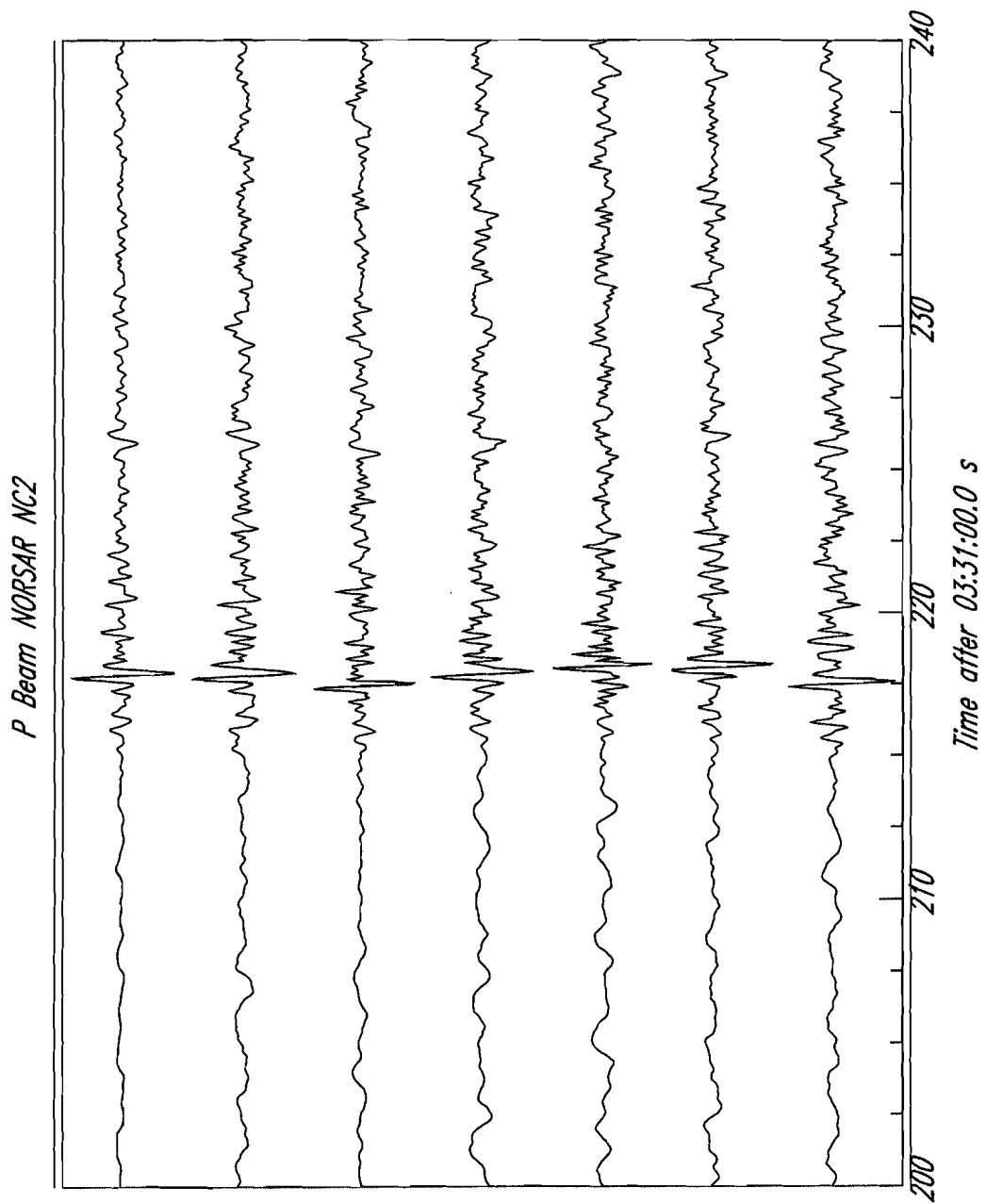


Figure A3d: As Figure A3a, except for NORSAR subarray NC2

*P Beam NORSAR NC3*

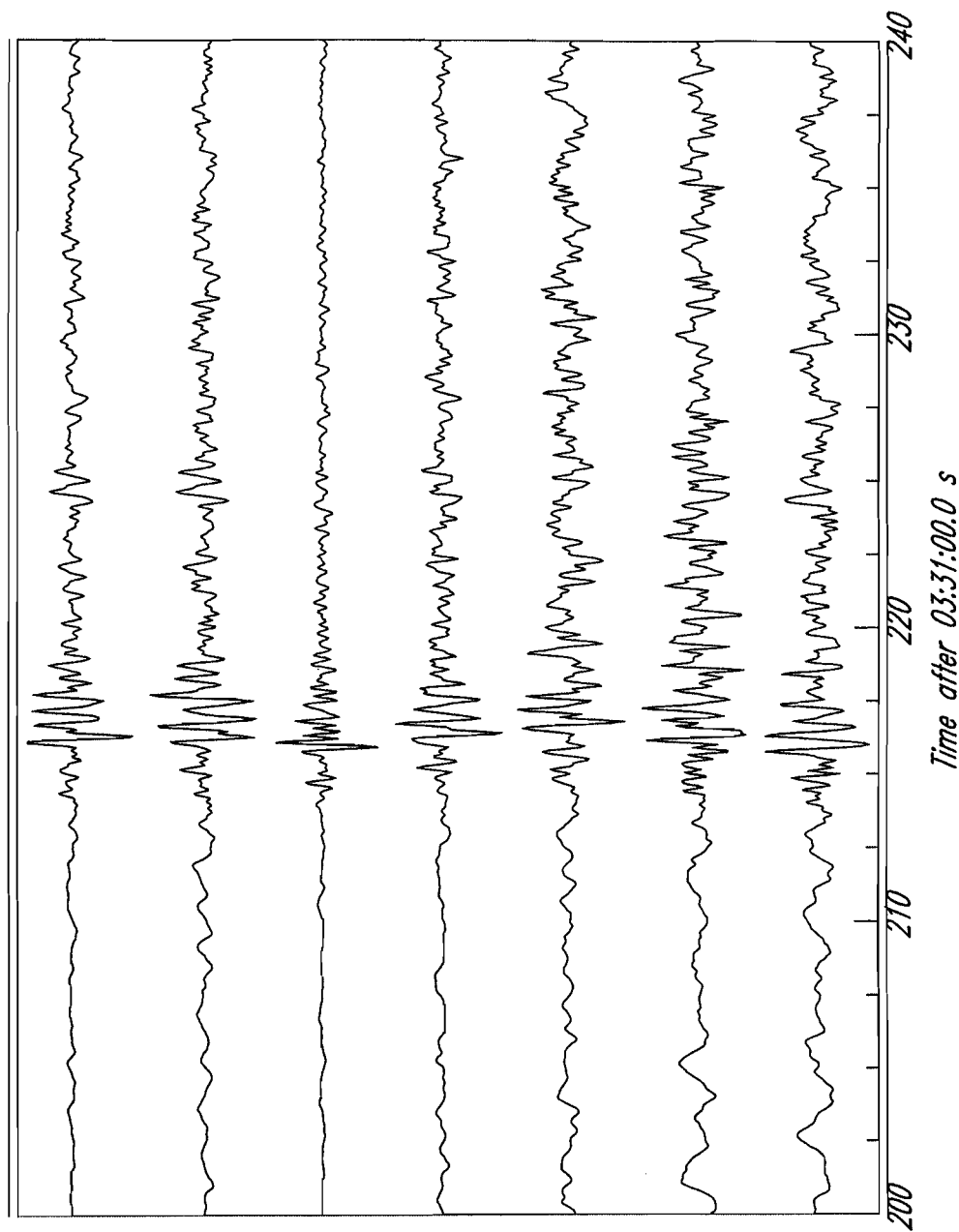


Figure A3e: As Figure A3a, except for NORSAR subarray NC3

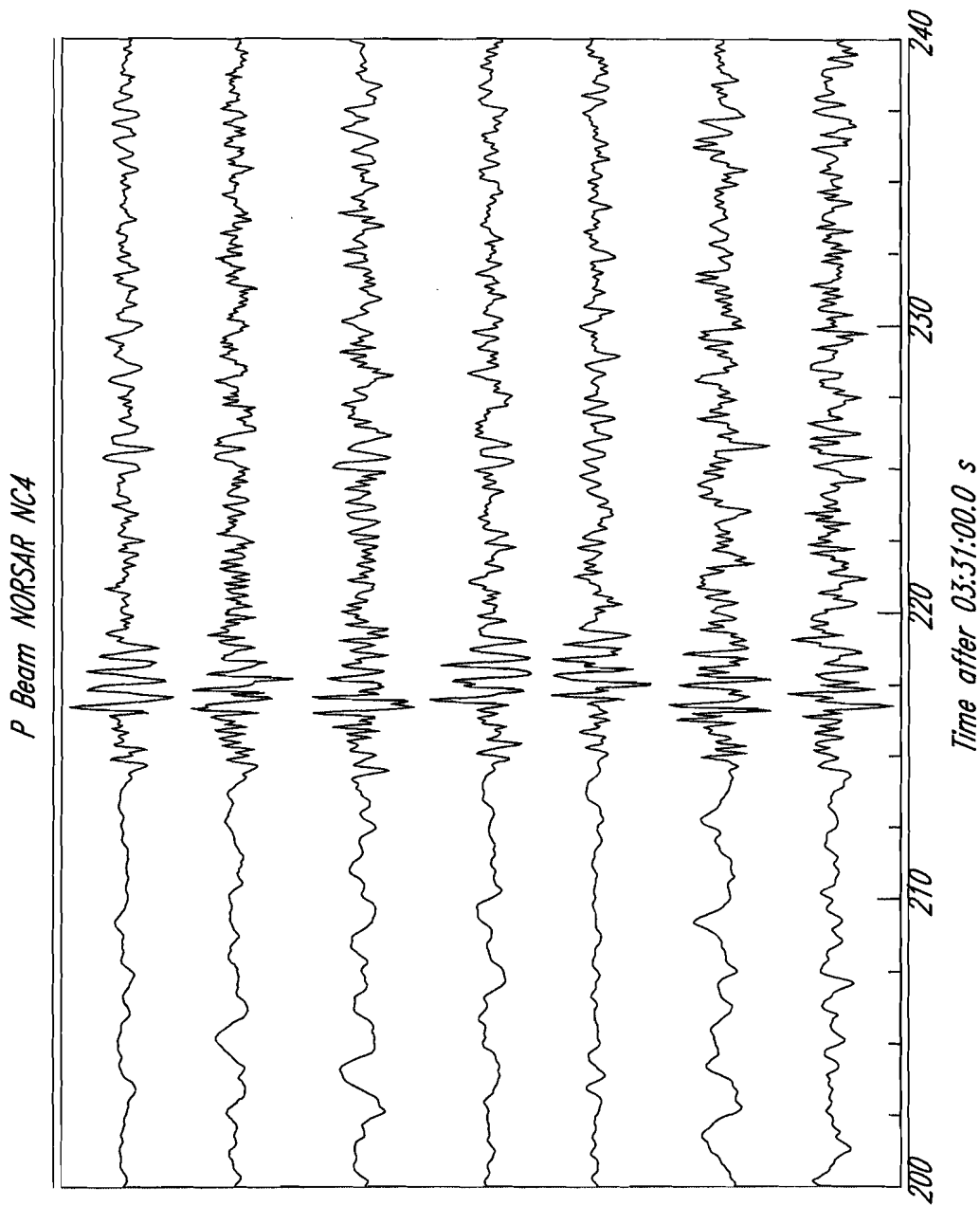


Figure A3f: As Figure A3a, except for NORSAR subarray NC4

*NC4.beam*  
 22.628  
*NC400*  
 49.625  
*NC401*  
 25.935  
*NC402*  
 41.449  
*NC403*  
 37.670  
*NC404*  
 24.318  
*NC405*  
 22.640

UK UNLIMITED

Available from

HER MAJESTY'S STATIONERY OFFICE

49 High Holborn, London W.C.1  
71 Lothian Road, Edinburgh EH3 9AZ  
9-12 Princess Street, Manchester M60 8AS  
Southey House, Wine Street, Bristol BS1 2BQ  
258 Broad Street, Birmingham B1 2HE  
80 Chichester Street, Belfast BT1 4JY  
or through a bookseller.

ISBN-0-85518210-5

Printed in England

© Crown Copyright 1998 MOD

UK UNLIMITED